

Baryons: What, When and Where?

Jason X. Prochaska and Jason Tumlinson

Abstract We review the current state of empirical knowledge of the total budget of baryonic matter in the Universe as observed since the epoch of reionization. Our summary examines on three milestone redshifts since the reionization of H in the IGM, $z = 3, 1,$ and 0 , with emphasis on the endpoints. We review the observational techniques used to discover and characterize the phases of baryons. In the spirit of the meeting, the level is aimed at a diverse and non-expert audience and additional attention is given to describe how space missions expected to launch within the next decade will impact this scientific field.

1 Introduction

Although baryons are believed to be a minor constituent of the mass-energy budget of our universe, they have played a dominant role in astronomy because they are the only component that interacts directly and frequently with light. Indeed, much of modern astrophysics focuses on the production and destruction of heavenly bodies comprised of baryons. Current observations of baryons extend from our Solar System to the very early universe ($z > 7$), i.e. spanning over 95% of the lifetime of our known universe. In terms of cosmology, the principal areas of baryonic research include measuring their total mass density, identifying the various elements and phases that comprise them, and resolving their distribution throughout the universe. In turn, astronomers are increasingly interested in probing the baryonic processes that feed galaxy formation and the feedback processes of galaxies that transform

Jason X. Prochaska
University of California Observatories - Lick Observatory, University of California, Santa Cruz,
CA 95064, e-mail: xavier@ucolick.org

Jason Tumlinson
Yale Center for Astronomy and Astrophysics, Yale University, P. O. Box 208121, New Haven, CT
06520, e-mail: jason.tumlinson@yale.edu

and return baryons to the intergalactic medium (IGM). Our mandate from the organizers was to review our knowledge of baryons to a broad astronomical audience from the epoch of reionization ($z \approx 6$) to the present day. Granted limited time, we focus on our empirical knowledge and limit the discussion of theoretical inquiry.

In the past two decades, advances in telescopes and instrumentation have significantly advanced our understanding the distribution of baryonic matter in the cosmos. Modern surveys of the local universe yield an increasingly complete census of galaxies and the large-scale structure in which they reside, the distribution of galaxy clusters and mass estimates of the hot gas within them, and a view of the diffuse gas that lies between galaxies. In this proceeding we review this work, placing particular emphasis on techniques related to observing diffuse baryonic phases. Presently these techniques are most efficiently pursued at $z \sim 3$ and $z \sim 0$, and observational constraints on the properties and distribution of baryons are most precise at these epochs. It is somewhat embarrassing that there lies a nearly 10 Gyr gap in our knowledge of the majority of baryons between these two epochs. Future missions need to address this hole in addition to the primary uncertainties remaining for the $z \sim 0$ and $z \sim 3$ epochs.

This proceeding is organized as follows: In § 2 we provide a basic introduction to the observational techniques used to trace baryons throughout the universe. The current best estimates for the total baryonic matter density is reviewed in § 3. We review the observational constraints on the main phases of baryons at $z = 3$ in § 4, briefly comment on our general absence of knowledge at $z = 1$ (§ 5), and then review the $z \sim 0$ missing baryons problem in § 6. We finish with a brief review of planned, proposed, and desired mission and telescopes that would significantly impact this science.

2 A Primer on Tracing Baryons

A complete baryon census poses a diverse set of observational challenges to astronomy, where we most often study baryons by observing the radiation that they emit, absorb or reflect. This includes stars, HII regions, cluster gas, planets, debris disks, etc. With these observations, one can assess the luminosity, temperature, chemical composition, and size of the object under study. In terms of performing a complete census and analysis of baryons in the present and past universe, however, this approach is currently limited by several factors. First, there is the simple fact that more distant objects are fainter. Although recent advances in telescopes, instrumentation, and search strategies now provide samples of galaxies at high redshift, these samples are sparse and (at $z > 1$) are comprised of only the brightest objects. There is no *a priori* reason why the budget of baryons would be dominated by the bright luminous objects, so these samples do not necessarily account for a large fraction of the budget. Second, it is generally difficult to estimate precisely the mass of an emitting object. With stars and galaxies, for example, mass estimates generally rely on stellar evolution modeling which is subject to many uncertainties (e.g. the initial

mass function) that are difficult to resolve even in the local universe. Third, it turns out that only a small fraction of the universe's baryons are in the collapsed, luminous objects that are most easily detected. This point is especially true in the young universe but it even holds in our modern universe. And finally, although diffuse gas emits line and continuum radiation, it is very difficult to detect this radiation even from gas in the nearby universe.

It is the last reason, in particular, that has driven observers to absorption-line techniques for characterizing the mass density, temperature, and distribution of the bulk of the baryons in the universe. The absorption-line experiment is standard observational astronomy in reverse: one observes a bright, background source (e.g. a quasar or gamma-ray burst) with the aim to study the absence of light due to absorption by intervening baryons. These basic analytic techniques were developed primarily to study the interstellar medium (ISM) of our Galaxy (e.g. [137]) via UV spectroscopy of bright O and B stars. Baryons with at least one electron will exhibit both resonant line absorption (e.g. Ly α) and continuum opacity (e.g. the Lyman limit feature), primarily at UV and X-ray frequencies. The principal observable of an absorption line is its equivalent width W_λ , the fraction of light over a spectral interval that is absorbed by the gas. The principal physical parameter is the column density N , the number of atoms per unit area¹ along the sightline. This is the number density equivalence of a surface density. For weak absorption, the column density scales linearly with the equivalent width. For stronger (i.e. saturated) lines, N depends weakly on W_λ and may be difficult to estimate. To assess these issues, it is highly desirable to obtain data at spectral resolution and to measure directly the optical depth profile of an absorption feature. In this manner, one can integrate the column density provided accurate knowledge of the atomic data of the transition.

Table 1 presents the principal absorption line features used to study H, He, and metals in diverse phases. Because most of these spectral features have rest wavelengths at ultraviolet or higher energies, one must utilize UV and X-ray telescopes to probe the past ≈ 7 Gyr of the universe (i.e. $z < 1$). These satellite missions have limited aperture and (often) low-throughput instrumentation which requires very bright background sources. Most of the gas, at least at $z > 1$, is relatively cool ($T \sim 10^4$ K) and the observed absorption lines have widths less than ≈ 40 km s⁻¹. To spectrally resolve such features, one is driven toward echelle spectrometers and generally the largest telescopes on Earth (or in space). In these respects the $z \sim 0$ absorption-line experiment is much more challenging than studies of the high z universe, where several of the key features are redshifted into optical pass-bands and accessible to large ground-based telescopes. This has led, in a few ways, to a greater understanding of baryons in the $z \sim 3$ universe than our recent past.

A tremendous advantage of the absorption-line experiment is that it achieves extremely sensitive limits for studying diffuse gas. For example, the signal-to-noise and resolution easily afforded by current telescopes and instrumentation allows detection of the HI Ly α transition to column densities $N_{\text{HI}} \sim 10^{12}$ cm⁻². This is ten

¹ Although we generally view stars and quasars as point sources, they have finite area. One may envision the concept of column density like a core sample of the Earth, where spectra resolve the location of gas in velocity not depth.

Table 1 Key Baryonic Diagnostic Lines and Features

Line	Phase	T (K)	λ_{rest} (Å)	$\lambda_{z=1}$ (Å)	$\lambda_{z=3}$ (Å)	$\lambda_{z=9}$ (μ)
Lyman-Werner	Molecular gas	10–100	~ 1000	2000	4000	1
21cm	Atomic gas	100–1000	21cm	0.7 GHz	0.4 GHz	140 MHz
Ly α	Atomic+Ionized gas	100–40000	1215	2400	4800	1.2
H α	Ionized gas	10000–40000	6560	13000	26000	65000
Lyman limit	Ionized gas	10000–40000	912	1800	3600	0.9
HeII	Ionized gas	10000–40000	225	450	912	0.2
CIV	Ionized Gas	20000–40000	1550	3000	6000	1.5
OVI	Warm/Hot Gas	20000– 10^6	1030	2000	4000	1
OVII,OVIII	Hot Gas	10^6 – 10^8	20	40	8	200

orders of magnitude lower than the surface density of a typical molecular cloud in a star-forming galaxy. With coverage of the full Lyman series, one can measure the surface density of atomic hydrogen across these ten orders of magnitude and probe the densest material to very diffuse environments. By the same token, one can study cold H₂ ($T < 100$ K) molecules through Lyman/Werner absorption bands while also probing diffuse, hot ($T > 10^6$ K) gas via metal-line transitions of O, N, and Ne. One thereby traces structures in the universe with a wide dynamic range of sizes: molecular clouds with diameters less than 100 pc in the centers of galaxies to ‘voids’ spanning tens of Mpc.

There are several disadvantages, however, to absorption-line studies: (1) the majority of key diagnostics have rest-frame UV or X-ray frequencies. At low z , one requires a space mission with large collecting area and efficient spectrometers to perform the experiment. This is expensive and often technologically infeasible; (2) One requires a bright, background UV/X-ray source² subjecting the final analysis to biases in the discovery and selection of these sources; (3) Bright UV/X-ray sources are rare and sparsely distributed across the sky. Therefore, multiplexing has limited value and observational surveys are relatively expensive. Furthermore, with only a limited number of sightlines to probe the universe, the densest (i.e. smallest) structure are at best sparsely sampled; (4) The technique is limited to the most distant luminous objects detected, currently $z \approx 6$; (5) dust intrinsic to the gas under study may extinguish the background source and preclude the analysis altogether.

Several key aspects of absorption-line research are illustrated in Figure 1 which presents the echelle spectrum of quasar J133941.95+054822.1 acquired with the Magellan/MIKE spectrometer [6]. This optical spectrum shows the rest-frame UV emission of the $z_{QSO} = 2.980$ quasar. One notes the broad Ly α +NV emission line superimposed on a underlying, approximately power-law spectrum. All of the absorption features, meanwhile, are associated with gas foreground to the quasar. The most prominent is the continuous opacity at $\lambda < 3600\text{Å}$ which marks the Lyman limit of a gas ‘cloud’ at $z_{LLS} = 2.97$. This Lyman limit system (LLS) must have

² Traditionally, researchers have used quasars although increasingly transient gamma-ray burst afterglows are analyzed (e.g. [21, 157]).

an HI column density $N_{\text{HI}} > 10^{17} \text{ cm}^{-2}$ to exhibit a Lyman limit opacity $\tau_{\text{LL}} > 1$. The thicket of narrow absorption lines at $\lambda = 3600$ to 4850 \AA is dominated by Ly α absorption from gas with $z < z_{\text{QSO}}$. These lines are termed the Ly α forest and they trace the intergalactic medium (IGM) of the high z universe. Their HI column densities are generally less than 10^{15} atoms per cm^2 . Within the Ly α forest one also notes a very broad absorption line at $\lambda \approx 4360 \text{ \AA}$ whose observed equivalent width is $W_\lambda \approx 50 \text{ \AA}$. This ‘redwood’ of the Ly α forest is a damped Ly α system (DLA); its very large HI column density, $N_{\text{HI}} > 2 \times 10^{20} \text{ cm}^{-2}$, allow the Lorentzian damping wings to be resolved in the Ly α transition. This feature marks the presence of a foreground galaxy and has a larger HI column density than total of all other lines in the Ly α forest. Finally, one observes a more sparse set of absorption features at $\lambda > 4900 \text{ \AA}$ which are metal-line transitions from ions and atoms of O^0 , Si^+ , C^+ , C^{+3} , Fe^+ , etc. These lines enable studies of the metal abundance of our universe [106, 126] and also probe gas phases that are difficult to examine with Ly α alone.

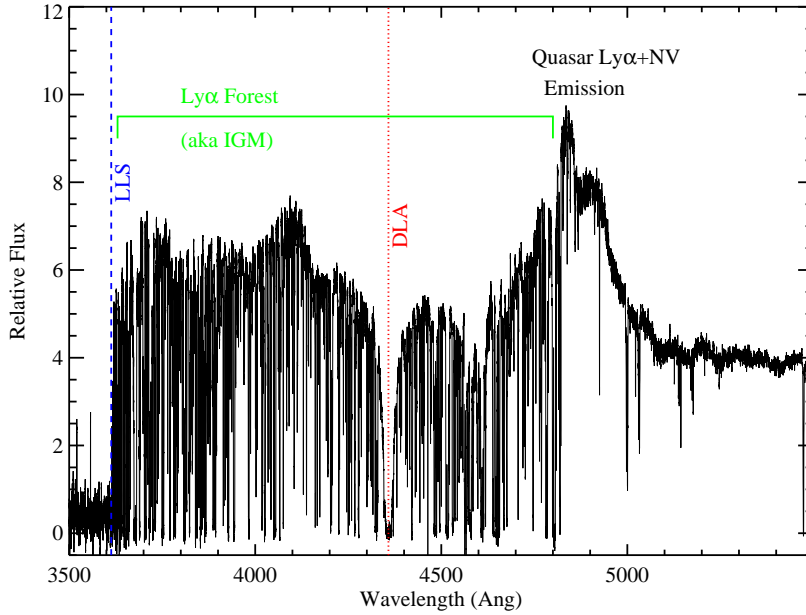


Fig. 1 Magellan/MIKE echelle spectrum of the $z_{\text{QSO}} = 2.980$ quasar J133941.95+054822.1. The data reveal the broad Ly α +NIV emission line of the quasar imposed on its otherwise nearly power-law spectrum. Imprinted on this spectrum is a plethora of absorption features due to gas foreground to the quasar. In particular, one identifies continuum opacity at $\lambda < 3600 \text{ \AA}$ due to a Lyman limit system at $z_{\text{LLS}} = 2.97$ and a thick of absorption features related to the Ly α forest. We also mark the damped Ly α profile at $\lambda \approx 4360 \text{ \AA}$ of a foreground galaxy ($z_{\text{DLA}} = 2.59$).

3 The Baryonic Mass Density

Our first problem is to assess the total budget of baryonic matter in the Universe, preferably by independent measurement. The baryonic mass density ρ_b , generally defined relative to the critical density $\rho_c = 9.21 \times 10^{-30} h_{70}^2 \text{ g cm}^{-3}$, $\Omega_b \equiv \rho_b / \rho_c$, is a fundamental cosmological parameter. The first successful method for estimating Ω_b is to compare measurements of isotopes for the light elements (H, D, He³, He⁴, Li) against predictions from Big Bang Nucleosynthesis (BBN) theory. The relative abundances of these isotopes are sensitive to the entropy of the universe during BBN, i.e. the ratio of photons to baryons. At first, observers focused on He even though Li and D are much more sensitive ‘baryometers’. This was because He/H was inferred from nearby emission-line galaxies where one could obtain exquisite S/N observations. It is now realized, however, that the precision of the inferred He/H ratio is limited by systematic uncertainties in the modeling of HII regions and the precision of the atomic data [94].

The tightest constraints on Ω_b using BBN theory come from direct measurements of the D/H ratio. Ideally this ratio is measured in a metal-poor gas to minimize the likelihood that D has been astrated by stars. The first detections of D, however, were from absorption-line studies in the metal-rich Galactic ISM [118]. These observations establish a lower limit to the primordial D/H value of $\approx 1 \times 10^{-5}$ (e.g. [84]). In the past decade, echelle spectrometers on 10m-class telescopes have extended the experiment to high redshift [16]. Researchers have searched for the very rare ‘clouds’ which are metal-poor and therefore minimally astrated, have large HI column density, and are sufficiently quiescent that the higher order lines DI and HI Lyman series are resolved (the velocity separation is 82 km s^{-1}). Figure 2 shows a recent example. The first few transitions of the HI Lyman series are broadened by the damping wings of their ‘natural’ Lorentzian profiles and a fit to the profile establishes $N_{\text{HI}} = 10^{20.67} \text{ cm}^{-2}$. The DI transitions are lost within the cores of these strong absorption lines but higher order lines show resolved and unsaturated DI absorption. Analysis of these lines provide a precise estimation of the DI column density.

The D/H ratio is estimated from the $N(\text{DI})/N(\text{HI})$ ratio under the reasonable assumption that these isotopes have identical ion configurations³ and differential depletion. Allowing for these assumptions, the estimation of D/H is direct: abundances measurements from absorption-line studies are simply a matter of counting atoms. Unlike most other methods to measure abundances, the results are essentially independent of the local physical conditions in the gas. Figure 3 presents the ‘gold-standard’ set of D/H measurements from quasar absorption line surveys of high z , metal-poor absorbers. The observations are scattered about $\log \text{D/H} = -4.55$ with a boot-strap dispersion of 0.04 dex. Adopting standard BBN theory, this constrains $\eta \equiv n_b/n_\gamma = 5.8 \times 10^{-10}$ where n_b and n_γ are the number densities of baryons and photons respectively. Direct measurements of the cosmic microwave background give n_γ , and one derives a baryonic matter density relative to the critical density ρ_c , $\Omega_b = \rho_b/\rho_c = (0.043 \pm 0.003)h_{70}^{-2}$. It is a triumph of the BBN theory and observa-

³ The gas is self-shielding and likely has a high neutral fraction.

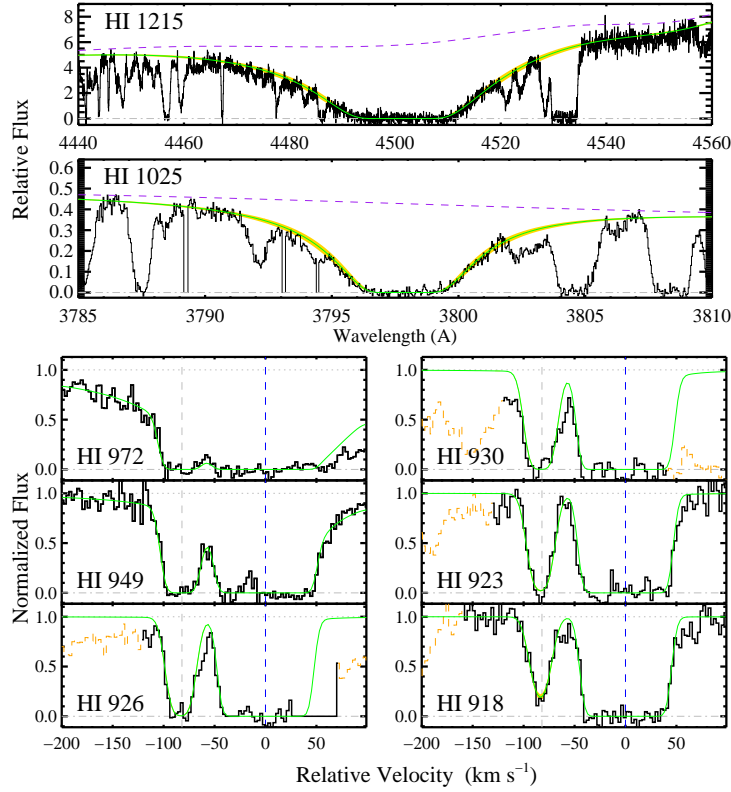


Fig. 2 H I and D I Lyman series absorption in the $z = 2.70262$ DLA towards SDSS1558-0031. For the $\text{Ly}\alpha$ and $\text{Ly}\beta$ transitions, the data is unnormalized and the dashed line traces the estimate for the local continuum level. The remaining Lyman series transitions are shown continuum normalized. The solid green line shows the best single-component fit to the D I and H I absorption. The estimate of the H I column density comes from analysis of the damping wings present in the Lyman α - δ lines whereas constraints on the D I column density come from the unsaturated D I Lyman-11 transition ($\sim 918 \text{ \AA}$ rest wavelength).

tional effort that this value has been confirmed by observations of the CMB power spectrum [36, 88].

Nevertheless, a few outstanding issues remain. The dispersion in D/H at high z exceeds⁴ that predicted from the reported errors on the individual measurements [70]. Although this most likely reflects over-optimistic error estimates by the observers, it is worth further exploring models of inhomogeneous BBN [57] and systematic error associated with the astrophysics of H and D [35]. The other outstand-

⁴ Interestingly, the same is true of the Galactic ISM measurements [60]. This result is unlikely to be due to observational error and the nature of the dispersion remains an open question [78, 109].

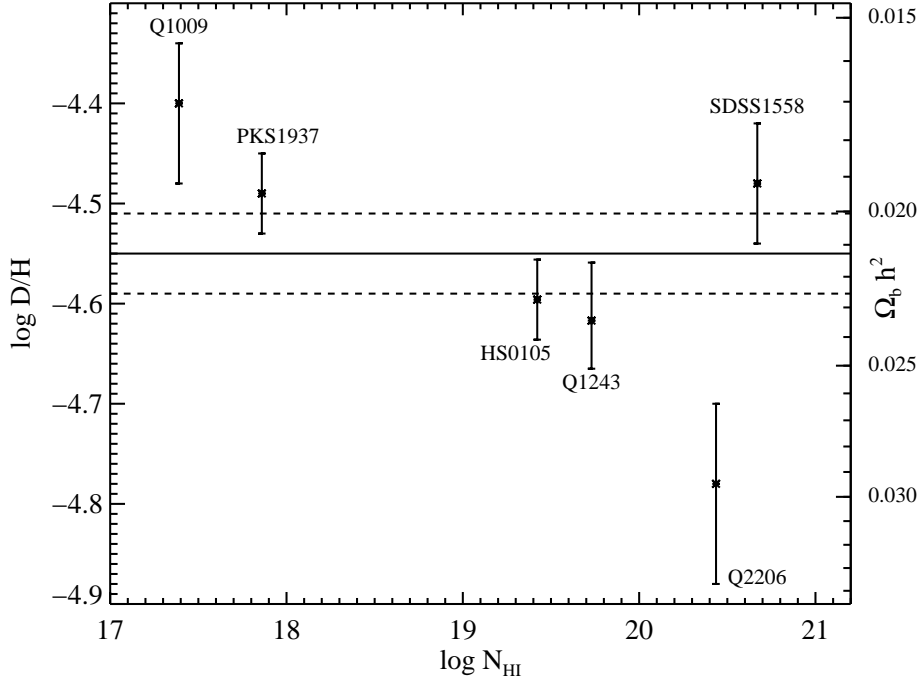


Fig. 3 Values of the D/H ratio vs. N_{HI} . The horizontal lines represent the weighted mean and jackknife errors of the 6 measurements, $\log D/H = -4.55 \pm 0.04$. The right hand axis shows how the values of D/H translate into values for $\Omega_b h^2$ using BBN.

ing issue concerns an inconsistency between the BBN-predicted Li abundance based on the η value from D/H and observation [9, 136]. It is now generally expected that this observed Li underabundance will be explained by non-primordial stellar astrophysics (e.g. [72]), but a comprehensive model of these processes has not yet been developed.

4 Baryons at $z \sim 3$

This section reviews constraints on the baryon census during the few Gyr following reionization, starting with the densest phases and proceeding to the least dense. Perhaps not coincidentally (for hierarchical cosmology), this organization also proceeds roughly from the lowest cosmological mass density to the largest. Along the way, we highlight the key uncertainties in these values and comment on the impact of future missions.

4.1 *The Stellar Component*

The majority (but not all) of galaxy samples identified at $z > 2$ are discovered through spectral or photometric signatures associated with ongoing star-formation. These include the Lyman break galaxies (see Shapley’s presentation), the Ly α emitters (e.g. [47]), sub-mm galaxies [19], and gamma-ray burst host galaxies (e.g. [76]). These populations dominate star formation activity during the young universe. It is likely that they also dominate the stellar mass density in this epoch because ‘red and dead’ galaxies are very rare at this time (e.g. [73]). It is difficult, however, to estimate the stellar mass density of these star-forming galaxies. This is especially true when one is limited to optical and near-IR photometry which corresponds to rest-frame UV and blue light, i.e. photons from massive star formation that provide little, if any, information on the low-mass end of the IMF.

To infer the stellar mass, one must adopt a mass to light ratio (M_*/L). Standard practice is to model the stellar population that gives rise to the photometry and spectroscopy of the galaxy. This modeling is sensitive to the presumed star-formation history, reddening by dust intrinsic to the galaxy, and uncertainties in the initial mass function. Altogether, these lead to large systematic uncertainties in the stellar mass estimate. These issues aside, current surveys do not probe the fainter galaxies of what appears to be a very steep luminosity function (e.g. [113]). The contribution by Dickinson provides a deeper discussion of these issues. Current estimates of the stellar mass density at $z = 3$ range from $\Omega_* = 2$ to $4 \times 10^{-7} h_{70} M_\odot \text{Mpc}^{-3}$ with a systematic uncertainty of $\approx 50\%$ [41, 120]. This corresponds to $0.005 \pm 0.002 \Omega_b h_{70}$. The launch of new satellites with greater sensitivity in near and mid-IR pass-bands (Herschel, JWST) will reduce the uncertainties by observing the stellar component at redder wavelengths and also by extending surveys to much fainter levels. Even with the large current uncertainty, however, it is evident that stars make a nearly negligible contribution to the total baryon budget at these redshifts.

4.2 *Molecular Gas*

In the local universe, star formation is associated with molecular gas in the form of molecular clouds. Although the link between molecular gas and star formation has not been extensively established at $z \sim 3$, it is reasonable to expect that the large SFR density observed at this epoch implies a large reservoir of molecular gas within high z galaxies (e.g. [54]). Indeed, molecular gas is detected in CO emission from a number of $z > 2$ galaxies [141, 158]. The observations focus on CO and other trace molecules because the H₂ molecule has no dipole moment and therefore very weak emission lines. Unfortunately, current millimeter-wave observatories do not afford extensive surveys for CO gas in high z galaxies. The Large Millimeter Telescope (LMT) and, ultimately, the Atacama Large Millimeter Array (ALMA) will drive this field wide open. These facilities will determine the CO masses for a large and more representative sample of high z galaxies and (for a subset) map out the spatial

distribution and kinematics of this gas. Similar to the local universe, to infer the total molecular gas mass from these CO measurements one must apply a CO to H₂ conversion factor, the so-called ‘X-factor’. The X-factor is rather poorly constrained even in the local universe and nearly unconstrained at high z . Therefore, a precise estimate of the molecular component at high z will remain a challenging venture.

Although observations of H₂ in emission are precluded at high redshift, the H₂ molecule does exhibit strong Lyman/Werner absorption bands in the rest-frame UV. These ro-vibrational transitions have large oscillator strengths and permit very sensitive searches for the H₂ molecule, i.e. H₂ surface densities of less than 10^{15} particles per cm². To date [48, 100], the search for H₂ has been targeted toward gas with a known, large HI column density ($N_{\text{HI}} > 10^{19}$ cm⁻²), i.e. the Lyman limit and damped Ly α systems. This is a sensible starting point; any sightline intersecting molecular gas in a high z galaxy would also be likely to intersect the ambient ISM of that galaxy and exhibit a large HI column density. Although present surveys are small, it is evident that the molecular fraction in these HI absorbers is very low. The frequency of positive detections is $\approx 15\%$ [90] and the majority of these have molecular fractions $f(\text{H}_2) < 10^{-3}$ [77]. Only a handful of these galaxies show molecular fractions approaching the typical Galactic values of even diffuse molecular clouds, $f(\text{H}_2) \sim 0.1$, along sightlines with comparable HI column density [25].

In hindsight the paucity of H₂ detections, especially ones with large $f(\text{H}_2)$, is not surprising. The formation of H₂ clouds represents a transition from the atomic phase, one that leads to gas with much lower T and much higher density. Consequently, cold molecular clouds phase exhibit much lower cross-section than when the gas is atomic. In turn, these clouds will have significantly lower probability of being detected by absorption line surveys. Analysis of the distribution of molecular gas in the local universe suggests that fewer than 1 in 1000 quasar sightlines should pierce a cold, dense molecular cloud [168]. In addition to this probabilistic argument, these clouds generally have very high dust-to-gas ratios and correspondingly large extinction. Therefore, even in the rare cases that a quasar lies behind the molecular cloud of a high z galaxy, it may be reddened and extinguished out of the optical, magnitude-limited surveys that dominate quasar discovery. It is somewhat curious, however, that GRB afterglow spectra also show very low molecular fractions in gas that is believed to lie very near star-forming regions [151].

In summary, there are very limited current constraints on the mass density and distribution of molecules in the young universe. Furthermore, future studies will focus primarily on tracers of H₂ and will also be challenged to precisely assess this very important phase. At present, our best estimate for the molecular mass density may be inferred from the atomic and stellar phases. Allowing for an order of magnitude uncertainty, we can estimate $\Omega_{\text{H}_2} = (0.001 - 0.1)\Omega_b$. Therefore, we suggest that the molecular phase contributes less than 10% of the mass density budget at $z \sim 3$.

4.3 Neutral Hydrogen Gas

In the local universe, galaxies have roughly equal measures of molecular and atomic hydrogen gas. The latter phase is primarily studied through 21-cm emission line surveys using large radio telescopes. Unfortunately, these radio telescopes do not have enough collecting area to extend 21-cm emission-line observations beyond $z \approx 0.2$ [75]. Although one can trace the 21cm line in absorption to much greater redshifts (e.g. [14, 62]), detections are exceedingly rare. This is due in part to the paucity of bright background radio sources and in part because galaxies have a relatively low cross-section of cold, neutral gas. For these reasons, neutral hydrogen gas at high z is principally surveyed via $\text{Ly}\alpha$ absorption. A total HI column density of $\approx 10^{20} \text{ cm}^{-2}$ is required for self-shielding to maintain neutral gas against the extragalactic UV background and local UV sources [155]. At these column densities, the damping wings of the $\text{Ly}\alpha$ transition are resolved even with moderate spectral resolution ($\text{FWHM} \approx 2\text{\AA}$; Figure 1). This spectral feature lends the name ‘damped $\text{Ly}\alpha$ system’ to the absorbers with $N_{\text{HI}} \geq 2 \times 10^{20} \text{ cm}^{-2}$.

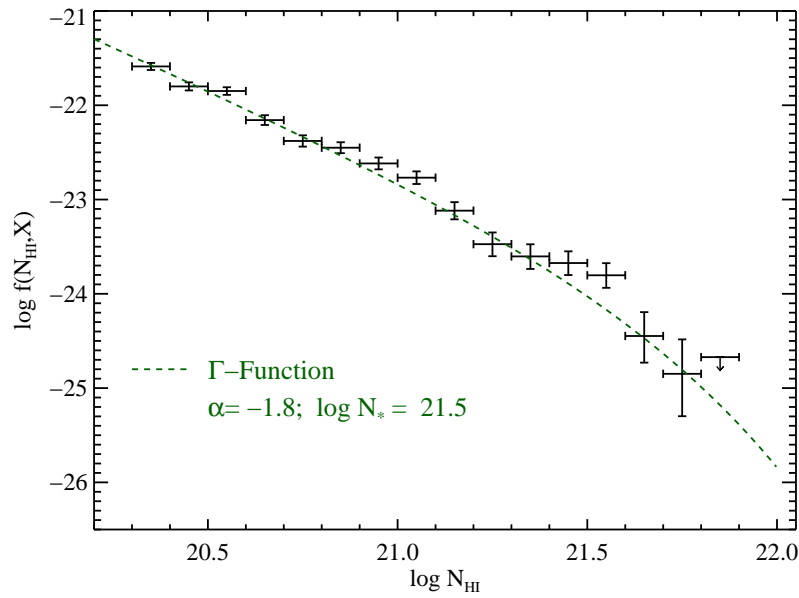


Fig. 4 The HI frequency distribution $f(N_{\text{HI}}, X)$ for the damped $\text{Ly}\alpha$ systems identified in the SDSS-DR5 quasar database (mean redshift $z = 3.1$). Overplotted on the discrete evaluation of $f(N_{\text{HI}}, X)$ is the best fitting Γ -function which is a reasonable (albeit unphysically motivated) description of the observations.

Wolfe and collaborators pioneered damped $\text{Ly}\alpha$ research beginning with the Kast spectrometer on the 3m Shane telescope at Lick Observatory [163, 164]. These op-

tical observations cover redshifts $z > 1.7$ which shifts Ly α above the atmospheric cutoff. The most recent DLA surveys leverage the tremendous public database of quasar spectroscopy from the Sloan Digital Sky Survey (SDSS; [1]). Figure 4 presents the frequency distribution $f(N_{\text{HI}}, X)$ of N_{HI} values per dN_{HI} interval per absorption pathlength dX for 719 damped Ly α systems identified in the SDSS-DR5 database (see <http://www.ucolick.org/~xavier/SDSSDLA>; [107]). This distribution function, akin to the luminosity function of galaxies, is reasonably well described by a Gamma function with a ‘faint-end slope’ $\alpha = -2$ and a characteristic column density $N_* \approx 10^{21.5} \text{ cm}^{-2}$. The first moment of $f(N_{\text{HI}}, X)$ yields the mass density of

neutral gas $\Omega_{\text{neut}}(X)dX \equiv \frac{\mu m_{\text{H}} H_0}{c \rho_c} \int_{N_{\text{min}}}^{\infty} N_{\text{HI}} f(N_{\text{HI}}, X) dX$ where μ is the mean molecular mass of the gas (taken to be 1.3), N_{min} is the column density which marks the transition from neutral to ionized gas (taken here as $10^{20.3} \text{ cm}^{-2}$), H_0 is Hubble’s constant, and ρ_c is the critical mass density. The faint-end slope of $f(N_{\text{HI}}, X)$ is logarithmically divergent, but the break at N_* gives a finite density.

Current estimates for Ω_{neut} from the SDSS-DR5 database give $\Omega_{\text{neut}} = 0.016 \pm 0.002 \Omega_b$. There is a modest decline by a factor of ≈ 2 from $z = 4$ to $z = 2$ where the latter value is (remarkably) in agreement with the neutral gas mass density observed today (§ 6.3). One may speculate, therefore, that the neutral gas mass density has been nearly invariant for the past ≈ 10 Gyr (but see [111]). This mild evolution aside, we conclude that the neutral, atomic gas phase at $z = 3$ comprises only $\simeq 1 - 2\%$ percent of the baryon budget at high z . Cosmological simulations suggest that this gas comprises the ISM of galaxies in formation, an assertion supported by measurements of DLA clustering with bright star-forming galaxies [11, 24] and the detection of heavy elements in all DLAs [106]. We can conclude that the sum of galactic baryonic components is a minor fraction ($< 10\%$) of the total baryonic mass density at $z \sim 3$. This is, of course, a natural consequence of hierarchical cosmology (e.g. [87]).

With the DLA samples provided by the SDSS survey, the statistical error on Ω_{neut} approaches 10% in redshift bins $\Delta z = 0.5$. At this level, systematic errors become important, especially biases associated with the selection criteria and magnitude limit of optically bright quasars. The bias which has received the most attention is dust obscuration [38, 92], i.e. dust within DLAs redden and extinguish background quasars removing them from optical surveys. The dust-to-gas ratio in the ISM of these high z galaxies is small [86, 102, 156], however, and the predicted impact on Ω_{neut} is only of the order of 10%. This expectation has been tested through DLA surveys toward radio-selected quasars [37, 61], which show similar results, albeit with poorer statistical power.

Although we would like to extend estimates of Ω_{neut} to $z > 5$, the experiment is challenged by the paucity of bright quasars (although this may be overcome with GRB afterglows) and because the collective, blended opacity of gas outside of galaxies (i.e., the IGM) begins to mimic damped Ly α absorption. By $z = 6$, the mean opacity of the universe approaches unity at Ly α [161] and the experiment is entirely compromised. Of course, current expectation is that the universe is predominantly neutral not long before $z = 6$, i.e. $\Omega_{\text{neut}} = \Omega_b$. These expectations and the evolution

of neutral gas at $z > 6$ will be tested through 21 cm studies of the young universe (see contributions by Furlanetto and Loeb for discussions of this reionization epoch).

4.4 Ionized Gas

As Figure 6 indicates, the mass densities of stars, molecular gas, and neutral gas are unlikely to contribute significantly to Ω_b at $z \sim 3$. Unless one invokes an exotic form of dense baryonic matter (e.g. compact objects), the remainder of baryons in the early universe must lie in a diffuse component outside of the ISM of galaxies. Indeed, the absence of a complete Gunn-Peterson trough in $z < 6$ quasars demonstrates that the majority of baryons are highly ionized at these redshifts. Because it is impossible to directly trace H^+ , we must probe this phase through the remaining trace amounts of HI gas or, in principle, HeI and HeII. Unfortunately, the resonance-line transitions of He have wavelengths that preclude easy detection (Table 1; though the Gunn-Peterson effect has been observed in HeII, see [74, 131]). Therefore, the majority of research has focused on the frequency distribution of HI column densities for gas associated with the IGM (a.k.a. the Ly α forest).

The modern description for the Ly α forest is an undulating density fields with minor, but important peculiar velocities and temperature variations. In this paradigm, it may be more fruitful to assess distribution functions of the smoothly varying optical depth of the IGM [4, 40, 67, 79] and compare these against theoretical models [10, 83]. Nevertheless, the classical approach of discretizing the Ly α forest into individual absorption lines does yield valuable insight into the distribution and mass density of baryons in the intergalactic medium. This analysis is generally summarized through the distribution function of HI column densities, $f(N_{\text{HI}}, X)$. Figure 5 summarizes our current knowledge of the $f(N_{\text{HI}}, X)$ distribution for both the ionized and neutral gas. Quasar absorption line analysis to date has provided an assessment of $f(N_{\text{HI}}, X)$ from $N_{\text{HI}} = 10^{12}$ to 10^{22} cm^{-2} with an important gap spanning from $N_{\text{HI}} \approx 10^{15-19} \text{ cm}^{-2}$. At column densities larger than 10^{22} cm^{-2} , the systems are too rare to be measured with existing quasar samples. Detections below 10^{12} cm^{-2} are limited by S/N and by the difficulty of distinguishing absorption from single ‘clouds’ from unresolved blends of weaker and stronger lines (e.g. [69]).

Let us focus first on the systems exhibiting the largest N_{HI} values, the super Lyman limit systems (SLLS; also referred to as sub-DLAs). These absorbers are defined to have $10^{19} \text{ cm}^{-2} < N_{\text{HI}} < 10^{20.3} \text{ cm}^{-2}$. Similar to the DLAs, one can measure the HI column densities of SLLS through fits to the damping wings of the Ly α profile although higher resolution spectroscopy is required [91, 97]. Current surveys indicate that $f(N_{\text{HI}}, X)$ flattens below $N_{\text{HI}} \approx 10^{20} \text{ cm}^{-2}$ with $d \log f / d \log N \approx -1.4$ [91]. If the SLLS are predominantly neutral, then they would contribute only a few percent to Ω_{neut} and a negligible fraction of Ω_b (Figure 6). Most of these absorbers, however, are partially ionized with mean ionization fraction $\langle x \rangle \approx 0.9$ [98, 103]. In Figure 6 we display the baryonic mass density of the SLLS inferred from the HI frequency distribution and assuming an N_{HI} -weighted, average ionization fraction

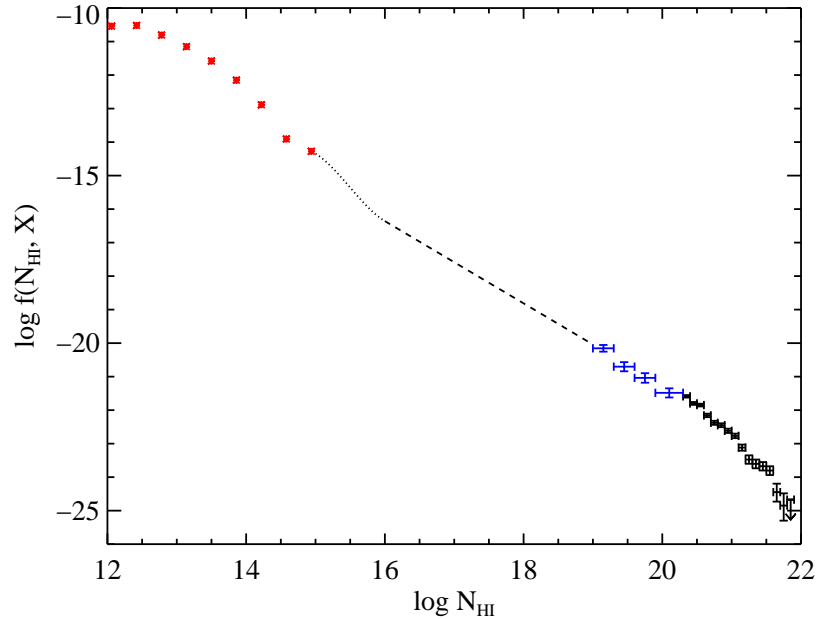


Fig. 5 The $f(N_{\text{HI}}, X)$ distribution function of ionized $N_{\text{HI}} < 10^{20} \text{ cm}^{-2}$ and neutral $N_{\text{HI}} > 10^{20} \text{ cm}^{-2}$ at $z = 3$. The data points at $N_{\text{HI}} \geq 2 \times 10^{20} \text{ cm}^{-2}$ correspond to the damped $\text{Ly}\alpha$ systems and are drawn from the SDSS-DR5 analysis of [107]. The data at $19 < \log(N_{\text{HI}}/\text{cm}^{-2}) < 20.3$ correspond to the super Lyman limit systems (SLLS) and were drawn from the analysis of [91]. The dashed line traces their best guess at the frequency distribution for the Lyman limit systems with $16 < \log(N_{\text{HI}}/\text{cm}^{-2}) < 19$. For the $\text{Ly}\alpha$ forest ($N_{\text{HI}} < 10^{15} \text{ cm}^{-2}$) we adopt the results from [69] normalized to our assumed cosmology [135]. Finally, the dotted line is a spline fit to the $\text{Ly}\alpha$ forest data and the functional form for the LLS given by [91]. Although the turnover in $f(N_{\text{HI}}, X)$ at $N_{\text{HI}} < 10^{13.5} \text{ cm}^{-2}$ may be partially due to incompleteness, it is likely a real effect (see also [56, 68]).

$\langle x \rangle = 0.9$. We infer that the SLLS contribute on the order of 2% of the baryonic mass density at $z = 3$. The majority of the baryons must reside in yet more diffuse and highly ionized gas.

At column densities $N_{\text{HI}} = 10^{16}$ to 10^{19} cm^{-2} (the Lyman limit systems; LLS), the majority of the Lyman series lines are saturated and the damping wings of $\text{Ly}\alpha$ are too weak to measure. For these reasons, it is difficult to estimate N_{HI} values in this interval. In principle, one can precisely measure N_{HI} values for the partial Lyman limit absorbers with $N_{\text{HI}} < 10^{17} \text{ cm}^{-2}$ whose opacity at the Lyman limit is $\tau_{912} \approx 1$. To date, however, only small samples from heterogeneous surveys exist in this range of N_{HI} (e.g. [101]). Because the Lyman limit feature is easily identified, one more easily derives an integral constraint on $f(N_{\text{HI}}, X)$ by surveying the incidence of LLS in quasar spectra $\ell(X) = \int f(N_{\text{HI}}, X) dN_{\text{HI}}$ (e.g. [139]). This integral constraint includes gas with $N_{\text{HI}} > 10^{19} \text{ cm}^{-2}$, but is dominated by absorbers with low N_{HI} values. Current estimates indicate $\ell(X) = 7.5$ at $z = 3$ [99]. Analysis of the

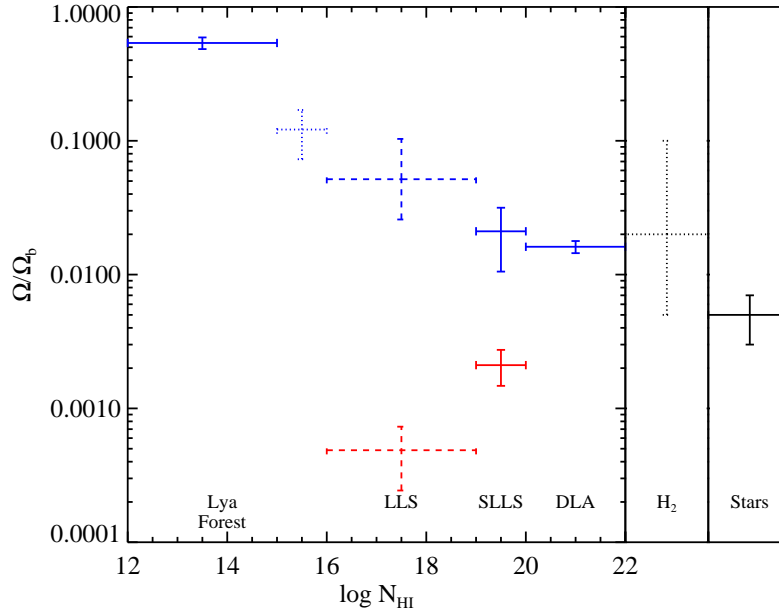


Fig. 6 Estimates of the baryonic mass density (relative to Ω_b) for various phases of baryons in the $z = 3$ universe. On the right side of the figure we show the stellar mass density estimate from several recent works [41, 120]. The uncertainty in this measurement is dominated by uncertainties in stellar population modeling and the presumed IMF. The phases corresponding to $\log N_{\text{HI}} < 22$ refer to absorption line systems traced by HI gas. The molecular gas content is very crudely estimated to lie near the stellar and atomic mass densities. The neutral atomic phase is traced by the DLAs where one estimates a mass density on the order of 1 to 2% Ω_b [107]. Gas with $N_{\text{HI}} < 10^{20} \text{ cm}^{-2}$ is predominantly ionized and one must make significant ionization corrections to estimate the mass density from the observed HI atoms. The red data points show the mass density from HI atoms alone for the LLS whereas the blue points represent estimates of the total mass density (see the text for details). The dashed symbols have weak empirical constraints and the dotted symbols have very weak empirical constraints.

SDSS database will greatly improve this estimate for $z > 3.2$ (O’Meara et al., in prep). Furthermore, complete analysis of the Ly α series for LLS will yield tighter constraints on $f(N_{\text{HI}}, X)$ within the interval $N_{\text{HI}} = 10^{17}$ to 10^{19} cm^{-2} (Prochter et al., in prep.). [91] combined the current observational constraints to predict $f(N_{\text{HI}}, X)$ across the LLS regime. These are presented as the dashed curve in Figure 5 and the uncertainty in this estimation is $\approx 50\%$.

Not only is $f(N_{\text{HI}}, X)$ very uncertain for the LLS, so too is the ionization state of this gas. For a few systems, analysis of metal-line transitions have confirmed the gas is predominantly ionized with ionization fractions $x > 0.95$ (e.g. [104]). The samples are too small, however, to reveal the distribution or trend of ionization fraction x with N_{HI} . Unfortunately, there is little insight from theory. Previous work with cosmological simulations has severely underestimated the incidence of Lyman limit systems (e.g. [46]) and it is likely that a careful treatment of radiative transfer is

required to assess these systems that are near the transition from neutral to ionized [71]. We can set a very conservative lower limit to their contribution by taking the $f(N_{\text{HI}}, X)$ function of O’Meara et al. and assume $x = 0$, $\Omega_{\text{LLS}} > 0.0004\Omega_b$. Ionization corrections will undoubtedly increase this limit by one or more orders of magnitude. Even in the case of a 100 times increase, it is very unlikely that LLS dominate the baryonic budget at $z \sim 3$. Figure 6 presents an estimate of the baryonic mass density of the LLS where we have adopted the HI frequency distribution presented in Figure 5 and estimated the ionization correction from simple Cloudy calculations assuming an ionization parameter $U = -2.5$, inferred from metal-line analysis of several LLS [104]. This implies a mass density estimate of $\approx 0.05\Omega_b$.

For column densities $N_{\text{HI}} \approx 10^{12}$ to 10^{15} cm^{-2} , where Ly β and/or Ly α are optically thin, the frequency distribution is reasonably well characterized by a power-law $f(N_{\text{HI}}, X) \propto N_{\text{HI}}^{-1.5}$ (e.g. [68, 69]). Observers do report, however, a departure from this power-law at $N_{\text{HI}} < 10^{13} \text{ cm}^{-2}$ which is likely not simply a consequence of incompleteness in the analysis [69]. Although the Ly α forest absorbers dominate the spectrum of any quasar by number, the total number of HI atoms that they contribute is negligible ($\approx 4 \times 10^{-6}\Omega_b$). From cosmological simulations of the high- z universe, we expect that the Ly α forest arises in undulating density fields of highly ionized gas filling large regions ($\approx \text{Mpc}$) with modest overdensity $\delta\rho/\rho \sim 3$. These same simulations argue that the majority of the baryonic mass density resides in the Ly α forest, with a contribution possibly exceeding $0.9\Omega_b$ (e.g. [15, 83]). Empirically, the gas is observed to only exhibit high-ion states of elements like C, Si, and O which demonstrate a high degree of ionization.

Because this gas is optically thin, if one can estimate its volume density and the intensity of the ionizing radiation field it is relatively straightforward to estimate its ionization fraction and thereby the total baryonic mass density of the Ly α forest. [124] has presented a simple but intuitive prescription for modeling the Ly α forest as gravitationally bound gas clouds whose size is of order the Jeans length. Within this prescription, which matches scaling laws derived from cosmological simulations, the ionization fraction x of the gas can be related to the HI column density:

$$x = 1 - 4.6 \times 10^{-6} \left(\frac{N_{\text{HI}}}{2 \times 10^{13} \text{ cm}^{-2}} \right)^{2/3} T_4^{-0.6} \Gamma_{12}^{-1/3} \quad (1)$$

where T_4 is the gas temperature in units of 10^4 K and Γ_{12} is the photoionization rate in units of 10^{-12} s^{-1} .

Photoionization should maintain the gas at a temperature near $2 \times 10^4 \text{ K}$, as predicted by the cosmological simulations. Within this prescription, therefore, the only major uncertainty is the ionization rate of the extragalactic UV background (EUVB) radiation field, Γ_{EUVB} . At $z = 3$, the EUVB will have contributions from both quasars and star-forming galaxies. The contribution of the former is directly measured from the luminosity function of $z = 3$ quasars. The contribution of galaxies, however, is far more uncertain. Although recent studies offer relatively well constrained UV luminosity functions (e.g. [113]), these are measured at $\lambda \approx 1500 \text{ \AA}$ in the rest frame, and so must be extrapolated to estimate the flux of ionizing photons.

Furthermore, one must adopt an escape fraction f_{esc} to estimate the flux emitted by these star-forming galaxies. Current empirical constraints are extremely limited [22, 129, 132]; the estimates range from $f_{esc} = 0$ to $\approx 10\%$. Because the comoving number density of star-forming galaxies greatly exceeds that of quasars, it is possible that galaxies contribute as much or more of the ionizing flux to the EUVB. Thus this ionizing background is uncertain at high redshift, with a corresponding uncertainty in the ionization correction for diffuse ionized gas.

The most conservative approach toward estimating the baryonic mass density of the Ly α forest is to assume $\Gamma_{EUVB} = \Gamma_{QSO}$. [55] provide an estimate of $\Gamma_{QSO} = 4.6 \times 10^{-13} \text{ s}^{-1}$ at $z = 3$ with an $\approx 30\%$ uncertainty. Convolving Equation 1 (assuming $\Gamma_{12} = 0.46, T_4 = 2$) with $f(N_{\text{HI}}, X)$, we infer a baryonic mass density $\Omega_{\text{Ly}\alpha} = 0.65\Omega_b$. Again, this should be considered a lower limit to $\Omega_{\text{Ly}\alpha}$ subject to the uncertainties of Equation 1. More detailed comparisons of the opacity of the Ly α forest with cosmological simulations reach a similar conclusion: the EUVB ionization rate exceeds that from quasars alone and $\Omega_{\text{Ly}\alpha} = 0.95\Omega_b$ (e.g. [58, 81, 83]). From a purely empirical standpoint, however, we must allow that as many as 20% of the baryons at $z = 3$ are still unaccounted for. It is very unlikely that the difference lies in photoionized gas with $N_{\text{HI}} < 10^{12} \text{ cm}^{-2}$ because the mass contribution of the Ly α forest peaks near $N_{\text{HI}} = 10^{13.5} \text{ cm}^{-2}$ [124]. Instead, one would have to invoke yet another phase of gas, e.g. hot diffuse baryons.

Ongoing surveys will fill in the current gap in $f(N_{\text{HI}}, X)$ for $N_{\text{HI}} = 10^{19} \text{ cm}^{-2}$ down to at least $N_{\text{HI}} = 10^{16.5} \text{ cm}^{-2}$. This gas, which likely is the interface between galaxies and the IGM, is very unlikely to contribute significantly to the baryonic mass density. It may be critical, however, to the metal mass density at $z \sim 3$ [12, 108]. Furthermore, the partial Lyman limits ($N_{\text{HI}} \sim 10^{17} \text{ cm}^{-2}$) dominate the opacity of the universe to HI ionizing radiation and therefore set the ‘‘attenuation length’’. This quantity is necessary to convert the observed luminosity function of ionizing radiation sources into an estimate of Γ_{EUVB} [51, 80]. These observations may also provide insight into the processes of reionization at $z > 6$ and the escape fraction of star-forming galaxies.

4.5 Hot Diffuse Baryons

In the previous section, we demonstrated that the photoionized IGM may contain all the baryons in the $z \sim 3$ universe that are not associated with dense gas and stars. We also noted, however, that this conclusion hinges on the relatively uncertain intensity of the EUVB radiation field. As a consequence even as much as $30\%\Omega_b$ may be unaccounted for in the IGM. One possible reservoir in this category is a hot ($T > 10^5 \text{ K}$) diffuse phase. Indeed, there are several processes already active at $z \sim 3$ that can produce a reservoir of hot and diffuse gas. The hard, intense radiation field from quasars and other energetic AGN processes (e.g. radio jets) may heat and ionize their surroundings out to several hundred kpc (e.g. [20]). Similarly, the supernovae that follow star formation may also drive a hot diffuse medium into the

galactic halo and perhaps out into the surrounding IGM (e.g. [2, 64]). Outflows of ionized gas are observed in the spectra of quasars and star-forming galaxies at these redshifts. On the other hand, gas accreting onto galactic halos is expected to shock heat to the virial temperature ($T > 10^6\text{K}$), especially in halos with $M > 10^{11}M_\odot$ [33]. Altogether these processes may heat a large mass of gas in and around high z galaxies.

Presently, there are very weak empirical constraints on the mass density and distribution of a hot, diffuse medium at $z \sim 3$. Detecting this gas in emission is not technically feasible and there are very few observable absorption-line diagnostics. difficult to trace, even with absorption-line techniques. The most promising approach uses the OVI doublet to probe highly ionized gas associated with the IGM (e.g. [5, 133]) and galaxies [42, 134]. These studies suggest a hotter component ($T > \sim 10^5\text{K}$) contributes on the order of a few percent Ω_b at $z \approx 2$.

The mass density of an even hotter phase ($\simeq 10^{6-7}\text{K}$), meanwhile, is unconstrained by observation. Ideally we would assess this component with soft X-ray absorption and/or emission but this will require a major new facility such as Con-X. We will take up these issues again in Section § 6.6 on the $z \sim 0$ universe, where the warm/hot component is predicted to be substantial.

Table 2 Empirical Summary of Baryons in the Universe

Phase	Temperature (K)	$\Omega(z=3)$		$\Omega(z=0)$	
		Location	Estimate ^a	Location	Estimate ^a
Stars	–	Galaxies	0.005 ± 0.002	Galaxies	0.06 ± 0.03
Molecular Gas	10^2	Galaxies	> 0.001	Galaxies	0.0029 ± 0.0015
Neutral Gas	10^3	Galaxies	0.016 ± 0.002	Galaxies	0.011 ± 0.001
Ionized Gas	10^4	IGM	> 0.80	IGM	$0.17^{+0.2}_{-0.05}$
Warm/Hot Gas	10^6	Galaxies?	> 0.01	Filaments?	??
Hot Gas	10^7	??	??	Clusters	0.027 ± 0.009

an assumed Ω_b value of 0.043.

5 Baryons in the $z \sim 1$ Universe

In contrast to the success that astronomers have had in probing baryons at $z \sim 3$, the knowledge of the distribution of baryons at $z \sim 1$ is quite limited. This is the result of several factors. One aspect is psychological: astronomers have pushed harder to study the universe at earlier times. This emphasis is shifting, however, with advances in IR spectroscopy (where the rest-frame optical diagnostics fall for $z \sim 1$), the impact of the Spitzer mission (e.g. Dickinson’s contribution), and the generation of large spectroscopic samples of $z \sim 1$ galaxies (GDDS, DEEP, VIRMOS). The other aspect is technical. As with the $z \sim 3$ universe, it is difficult or impossible with current facilities to build large samples of clusters to assess the host phase, or to survey

the molecular phase with CO, or to measure HI gas with 21-cm techniques. Furthermore, the majority of key absorption-line diagnostics (e.g. Ly α , CIV; Table 1) fall below the atmospheric cutoff and UV spectroscopy on space-based telescopes is necessary and expensive. Key emission-line diagnostics (H α , [OIII]), meanwhile, shift into the near-IR making it more difficult to pursue large galaxy surveys.

Surprisingly, the prospects are also limited for major advances in exploring baryons at $z \sim 1$ during the next decade. The notable positive examples are (i) Sunyaev-Zeldovich experiments, which should establish the mass function of $z \sim 1$ clusters, (ii) multi-object, near-IR spectrometers which will improve detections of star-forming galaxies and the luminosity function of early-type galaxies and (iii) the construction of mm telescopes (LMT, ALMA) that will enable surveys for molecular gas. These advances will allow astronomers to characterize the dense, baryonic component at $z \sim 1$. Similar to $z \sim 3$ and $z \sim 0$, however, we expect that these components will be minor constituents. It is a shame, therefore, that there is currently no funded path to empirically constrain the properties of diffuse gas, neutral or ionized. Upcoming ‘pathfinders’ for the proposed Square Kilometer Array (SKA) will extend 21-cm observations beyond the local universe but are unlikely to reach $z = 1$. This science awaits an experiment on the scale of SKA. The classical absorption-line experiments must access hundreds of faint QSOs at $z \simeq 1 - 2$ and so require a UV space mission probably on the scale of JWST [128]. At present, however, there is no development funding path toward such a mission. In this respect, our ignorance on the distribution and characteristics of the majority of baryons in the $z \sim 1$ universe may extend beyond the next decade.

6 Baryons in the $z \sim 0$ Universe

In this section, we follow closely the footsteps of [44], who presented a comprehensive census of baryons in the local universe (see [43] for an update). With this exercise in accounting, the authors stressed a startling problem: roughly 50% of the baryons in the local universe are missing! They further suggested that these missing baryons are likely hidden in a warm/hot ($T \approx 10^5$ to 10^7 K) diffuse medium that precluded easy detection. These claims were soon supported by cosmological simulations that predict a warm/hot intergalactic medium (WHIM) comprising 30 to 60% of today’s baryons [18, 30]. Motivated by these semi-empirical and theoretical studies, the search for missing baryons gained great attention and continues today. We review the current observational constraints on the distribution and phases of baryons in the local universe and stress paths toward future progress. As in previous sections, we roughly order the discussion from dense phases to the diffuse.

6.1 Stars

Large-area imaging and spectroscopic surveys (e.g., 2MASS, SDSS, 2dF) have precisely measured the luminosity function of galaxies in the local universe to faint levels [8, 23]. The light emitted by galaxies in optical and IR bands, therefore, is well characterized. Establishing the mass budget of baryons in these stars, however, requires translating the luminosity function into a mass function. The typical procedure is to estimate a stellar mass-to-light ratio (M/L) for each galaxy based on stellar population modeling of the colors of the integrated light. These estimates are sensitive to the metallicity, star-formation history, and (most importantly) the initial mass function (IMF) of star formation. Because the stellar mass of a galaxy is dominated by lower mass stars even at early times, the analysis is most accurately performed in red passbands.

The SDSS and 2dF galaxy surveys have led the way in this line of research; SDSS possesses the advantage of z -band imaging ($\lambda \approx 9000\text{\AA}$) which reduces the uncertainty in the M/L estimate. [63] analyzed the mass-to-light ratio for a large sample of SDSS galaxies, for which they report a luminosity function-weighted ratio $\langle M/L_z \rangle = 1.5$ with an uncertainty of $\approx 20\%$ and assuming a Kroupa IMF. Taking the [63] estimation of M/L with the SDSS luminosity function [8], [43] estimates a stellar mass density $\Omega_*(z=0) = 0.0025$, which includes an estimate of stellar remnants. Assuming a 50% uncertainty, we find $\Omega_*(z=0) = (0.06 \pm 0.03)\Omega_b$.

Further progress in estimating the stellar contribution to Ω_b is not limited by neither statistical error nor depth of the luminosity function, but rather by systematic uncertainty, especially in the IMF. [63] did not vary this assumption when estimating the error budget. Because sub-solar mass stars contribute most of the mass in stellar systems, uncertainties in the IMF can easily dominate the error budget. A conservative estimate of this uncertainty is $\approx 50\%$, especially if we allow for a Salpeter IMF.

The subject of stellar masses and their sensitivity to IMF is worthy of a review article in its own right, and so it is well beyond the scope of our mandate. Here we only pause to note three recent developments. First, the uncertainty in *total* stellar masses is probably only a factor of 1.5 - 2, even though the error may be larger for individual cases. Second, this topic is receiving more attention in stellar population synthesis models (e.g. Maraston, Bruzual and Charlot), which can now include IMF uncertainties in their budgets of systematic error. Finally, there have been recent, speculative suggestions that the IMF at high redshift may depart significantly from the Galactic form. At early times, generally hotter environments within galaxies and an elevated CMB may raise the typical stellar mass [29, 149, 154]. Though much theoretical work and experimental testing remains to be done in this area, it is possible that these ideas will ultimately lead to a more self-consistent picture of the evolution of stellar mass with redshift, with a consequent improvement in our understanding of the baryon budget. This is one of the key science goals of the JWST and ALMA facilities. These uncertainties aside, it is evident that stars are a sub-dominant baryonic component in our current universe. As an editorial aside, we note the irony that even the baryonic component that is easiest to see - the luminous

stars - is difficult to weigh. This uncomfortable fact should be kept in mind later as we attempt to assess the unseen, hot diffuse phases of the IGM.

6.2 Molecular Gas

With the exception of the Galaxy [122], the Magellanic Clouds [153], and some nearby starburst galaxies [53], there are very few direct detections of H_2 in the local universe. These detections are of absorption in the FUV Lyman-Werner bands, and so are accessible only in optically thin, essentially dust-less environments that are unlikely to contribute much to the total cosmic mass budget of molecular gas (judging from the Milky Way). Because it is a homonuclear molecule with no dipole moment, H_2 has only very weak quadrupole emission even if the density is high. The usual technique, then, is to track molecular gas with trace optically-thin species and infer the total molecular content through scaling factors calibrated against our Galaxy and others in the local universe. The most common indirect tracer is CO and its conversion factor is termed the ‘‘X-factor’’. In contrast with HI gas (see below), ‘blind’ surveys for CO have not yet been performed. Instead, researchers have estimated the molecular mass density by correlating CO mass with another galaxy observable (e.g. HI mass, infrared flux density) that has a well defined, volume-limited distribution function. The convolution of the two functions gives an estimate of the CO mass function [65, 165, 168]. Finally, this is converted to the H_2 mass function with the X-factor which is generally assumed to be independent of any galaxy properties. This latter assumption is known to be invalid for faint metal-poor galaxies and luminous starbursts, but variations are believed to be small for the $L \approx L_*$ galaxies that likely dominate the molecular mass density [34].

Taking $X \equiv N(\text{H}_2)/I(\text{CO}) = 3 \times 10^{20} \text{ cm}^{-2} (\text{K km s})^{-1}$ [165], [65] report $\Omega_{\text{H}_2} = \rho_{\text{H}_2} = 2.2 \times 10^7 h_{70} M_{\odot} \text{ Mpc}^{-3}$ for an IR sample of galaxies and [168] report $\Omega_{\text{H}_2} = 1.2 \times 10^7 h_{70} M_{\odot} \text{ Mpc}^{-3}$ for the optically selected BIMA sample. The factor of two difference in these estimates reflects the systematic error associated with sample selection. We adopt the mean value of the two estimates and assume a 30% uncertainty: $\Omega_{\text{H}_2} = 0.0029 \pm 0.0009 \Omega_b$. The next major advance for surveying molecular gas in the local universe awaits a wide-field, deep, and blind survey of CO gas with depth and area comparable to current 21-cm surveys. This is a difficult technical challenge and we know of no such survey that is currently planned.

6.3 Neutral Hydrogen Gas

Over the past decade, radio astronomers have performed blind surveys for 21-cm emission to derive the HI mass function of galaxies (e.g. [119, 166, 167]). The modern version is the HIPASS survey [82], an all Southern-sky survey for HI with the Parkes radio telescope. [167] present the HI mass function from HIPASS and

derive an integrated mass density $\Omega_{\text{HI}} = 3.8 \times 10^{-4} h_{70}^{-1}$. Including He, this implies a neutral gas mass density $\Omega_{\text{neut}} = (0.011 \pm 0.001) \Omega_b$. Although some uncertainty remains regarding the shape of the low-column (“faint-end”) slope for the HI mass function, the total mass density is dominated by $L \approx L_*$ galaxies. Another important result of these surveys is the demonstration that very little HI mass, if any, associated with star-free systems. Ultimately, the ongoing ALFALFA survey [49] will surpass the HIPASS sample in sensitivity and provide the definitive measure of the HI mass function at $z \sim 0$. In the future, facilities like the EVLA or Square Kilometer Array will be able to push such observations to $z \sim 1$ or beyond.

Interferometric observations can map the HI surface density profiles of low-redshift galaxies and thereby infer the HI frequency distribution at $N_{\text{HI}} > 10^{20} \text{ cm}^{-2}$ [121, 169]. This distribution function is illustrated in Figure 7. Remarkably, it has nearly identical shape to the $f(N_{\text{HI}}, X)$ function derived for $z \sim 3$ galaxies from damped Ly α observations (Figure 5). Both of these $f(N_{\text{HI}}, X)$ functions follow a roughly N_{HI}^{-2} power-law at lower column densities and exhibit a break at $\log N_{\text{HI}} \approx 21.7$. This suggests that HI gas is distributed in a similar manner within galaxies at $z \sim 0$ and $z \sim 3$. Perhaps even more remarkable is the fact that the integrated mass density is also very comparable. The Ω_{neut} value at $z \sim 0$ is at most three times smaller than the largest Ω_{neut} values derived from the $z \sim 3$ damped Ly α systems (0.0045 vs. 0.0014) and actually coincides with the Ω_{neut} value at $z = 2.2$ [107]. One might infer that Ω_{neut} has been constant for the past ≈ 10 Gyr, which suggests that all of the gas accreted into the neutral phase within galaxies is converted into stars (e.g. [66]).

6.4 Intracluster Medium (ICM)

The majority of galaxies in clusters are early-type with little or no neutral hydrogen gas. It may have been thought at first, therefore, that the baryonic content of clusters was almost entirely stars. X-ray observations, however, have revealed that clusters are filled with a hot plasma that extends to at least their virial radii (~ 1 Mpc). This intracluster medium (ICM) contains the baryons that have collapsed within the cluster structure and have been shock-heated to the virial temperature ($T > 10^7 \text{ K}$) of the cluster. Analysis of the X-ray surface brightness indicate that the ICM has an electron density profile $n_e(r) = n_0 [1 + (r/r_c)^2]^{3\beta/2}$ with $\beta \approx 0.6$ and n_0 ranging from 10^{-1} to 10^{-2} at r_c of a few hundred kpc (e.g. [114]). In fact the ICM mass significantly exceeds the stellar mass inferred for the galaxies within the cluster. From a cosmological standpoint, therefore, the ICM may represent a major baryonic component of our current universe.

Detailed analysis of the X-ray observations show that the gas fraction, f_{gas} , or the ratio of the gas mass to the dynamical mass, is nearly constant with cluster mass, $f_{\text{gas}} = 0.11 \pm 0.01$ [3]. Therefore, one can estimate the total baryonic mass density of the ICM in all clusters simply by taking the product of f_{gas} with the cosmological mass density of clusters. A recent estimation of the latter comes from an X-ray

selected sample of clusters with overlapping SDSS observations [117]. Fitting these data to the [59] dark-matter halo mass function for a WMAP5 cosmology [36], and integrating from high mass down to $M_{min} = 10^{14}M_{\odot}$, we derive a mass density of clusters, $\Omega_{cluster} = 0.010$. Adopting $f_{gas} = 0.11$, the ICM has a baryonic mass density $\Omega_{ICM} = 0.027\Omega_b$. Uncertainties in this estimate are dominated by the uncertainty in $\Omega_{cluster}$, which are in turn driven by uncertainty in the power spectrum normalization specified by σ_8 . These errors translate into a roughly 30% uncertainty in $\Omega_{cluster}$. This diffuse, hot component represents a non-negligible mass density in our modern universe. It raises the possibility that a similar medium associated with collapsed structures having $M < M_{min}$ (i.e. groups and isolated galaxies) could contribute significantly to the mass density of baryons at $z \sim 0$ [44, 85].

6.5 Photoionized Gas

Summing the mass densities for the gas and stars of the preceding sub-sections, we estimate a total mass density of only $\approx 0.10\Omega_b$. Similar to the high- z universe,

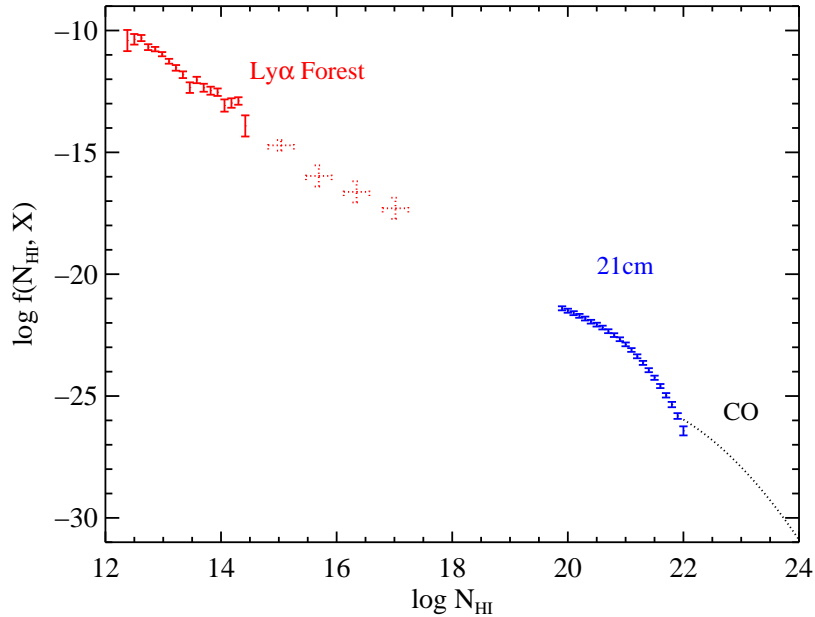


Fig. 7 The $f(N_{\text{HI}}, X)$ distribution function of ionized $N_{\text{HI}} < 10^{20} \text{cm}^{-2}$, neutral $N_{\text{HI}} = 10^{20-22} \text{cm}^{-2}$, and molecular $N_{\text{HI}} > 10^{22} \text{cm}^{-2}$ gas at $z \sim 0$. The data at $N_{\text{HI}} < 10^{17} \text{cm}^{-2}$ which correspond to HST/STIS observations of the low redshift Ly α forest are taken from [96], the distribution function neutral, atomic hydrogen gas is taken from 21cm WSRT observations [169], and the distribution function of molecular gas is estimated from BIMA CO observations [168].

therefore, we conclude that the majority of baryons at $z \sim 0$ lie in diffuse gas outside of virialized structures. It is reasonable to speculate first that the photoionized component, i.e. the intergalactic medium, is also the major baryonic reservoir at $z \sim 0$. As with the $z \sim 3$ universe, this component is best traced by Ly α absorption using UV absorption-line spectroscopy. Even a visual inspection of low- z quasar spectra shows that the incidence of Ly α absorption $\ell(X)$ is quite low relative to the $z \sim 3$ universe. This sharp decline in $\ell(X)$ is a natural consequence, however, of the expanding universe. Quantitatively, the decline in $\ell(X)$ is actually less than predicted from expansion alone [159] because of a coincident decrease in the EUVB intensity which implies a higher neutral fraction and correspondingly higher incidence of HI absorption [31].

The HI column density distribution function of the $z \sim 0$ IGM has been characterized by several groups using UV spectrometers onboard the Hubble Space Telescope [32, 96]. In Figure 7, we show the Penton et al. $f(N_{\text{HI}}, X)$ results for a sample with mean redshift $z = 0.03$. These results assume a Doppler parameter $b_{\text{IGM}} = 25 \text{ km s}^{-1}$ for all absorption lines identified in their survey. The results are insensitive to this assumption for low column densities ($N_{\text{HI}} < 10^{14} \text{ cm}^{-2}$) because the Ly α profiles are unsaturated but measurements at higher N_{HI} are sensitive to b_{IGM} and have much greater uncertainty. Similar to the $z \sim 3$ universe, the $f(N_{\text{HI}}, X)$ function is sufficiently steep that one expects the mass density is dominated by clouds with $N_{\text{HI}} < 10^{15} \text{ cm}^{-2}$. [96] have fitted the distribution function at low N_{HI} with a power-law function $f(N_{\text{HI}}, X) = AN_{\text{HI}}^{\beta}$ and report $A = 10^{10.3 \pm 1.0}$ and $\beta = -1.65 \pm 0.07$ with significant degeneracy between the two parameters.

We may estimate the IGM baryonic mass density at $z \sim 0$ using the formalism described in § 4.4 following [125]. In addition to $f(N_{\text{HI}}, X)$, this analysis requires an estimate of the HI photoionization rate Γ and the gas temperature T_{IGM} . The dependences of the mass density on these quantities are weak ($\Omega_{\text{Ly}\alpha} \propto \Gamma^{1/3} T^{3/5}$) but so too are the empirical constraints. Estimates of Γ range from 0.3 to $3 \times 10^{-13} \text{ s}^{-1}$ [127, 160] and we adopt $\Gamma = 10^{-13} \text{ s}^{-1}$ based on calculations of the composite quasar and galaxy background estimated by Haardt & Madau (CUBA; in prep). The characteristic temperature of the IGM is constrained empirically only through the observed distribution of line widths, b_{IGM} . Several studies report a characteristic line width at $z \sim 0$ of $b_{\text{IGM}} \approx 25 \text{ km s}^{-1}$ which implies $T_{\text{IGM}} < 75,000 \text{ K}$ [32, 93, 95]. This is an upper limit because it presumes the line widths are thermally and not turbulently, broadened. Indeed, [32] have argued from analysis of numerical simulations that the observed b_{IGM} distribution is in fact dominated by non-thermal motions. These same simulations suggest a density-temperature relation $T_{\text{IGM}} \approx 5000(\rho/\bar{\rho})^{0.6} \text{ K}$ (the so-called ‘‘IGM equation of state’’).

Combining $\Gamma = 10^{-13} \text{ s}^{-1}$ and the [32] $\rho - T$ ‘‘equation-of-state’’ with the [96] estimation for $f(N_{\text{HI}}, X)$ and the [125] formalism, we estimate the baryonic mass density of the $z \sim 0$ Ly α forest ($N_{\text{HI}} = 10^{12.5-14.5} \text{ cm}^{-2}$) to be $\Omega_{\text{Ly}\alpha} = 0.0075 = 0.017\Omega_b$. This is several times smaller than the mass density estimate for the IGM at $z \sim 3$ (Figure 6). The immediate implication is that the IGM may not be the majority reservoir of baryons at $z \sim 0$. Indeed, the missing baryons problem hinges on this result. It is crucial, therefore, to critically assess the uncertainty in this estimate, in

particular whether current observational constraints allow for a significantly larger value.

First, consider the photoionization rate Γ which is constrained to no better than a factor of a few (at any redshift). As noted above, $\Omega_{\text{Ly}\alpha}$ is largely insensitive to the photoionization rate ($\Omega_{\text{Ly}\alpha} \propto \Gamma^{1/3}$). Furthermore, our adopted value lies toward the upper end of current estimations which leads us to conclude that a more precise measure of Γ will not markedly increase the baryonic mass density inferred for the IGM at $z \sim 0$.

Another consideration is the temperature of the IGM, although again the mass density is not especially sensitive to this quantity. If the Ly α forest were uniformly at $T_{\text{IGM}} = 2 \times 10^4 \text{K}$ we would derive only a 50% higher baryonic mass density. It is evident that modifications to Γ and T_{IGM} will not make a qualitative difference in $\Omega_{\text{Ly}\alpha}$, though these effects in combination could increase it by a factor of 2. Turning to the HI frequency distribution, [96] and [32] emphasize that $f(N_{\text{HI}}, X)$ shows no break from a power-law down to the sensitivity limit of the HST/STIS observations, $N_{\text{lim}} = 10^{12.5} \text{cm}^{-2}$. It is reasonable, therefore, to extend the distribution function to lower column densities. Taking $N_{\text{lim}} = 10^{11.5} \text{cm}^{-2}$ with the power-law exponent fixed at $\beta = -1.65$, leads to a $2\times$ increase in $\Omega_{\text{Ly}\alpha}$. Finally, both cosmological simulations and some observational analysis suggest a steeper power-law ($\beta \approx -2$) [32, 93] which, in turn, may lead to an enhancement in $\Omega_{\text{Ly}\alpha}$. If we allow for a combination of these effects, it is possible to recover $\Omega_{\text{Ly}\alpha}$ values exceeding $0.5\Omega_b$. For example, the following parameter set – $\Gamma = 10^{-13} \text{s}^{-1}$, $T_{\text{IGM}} = 2 \times 10^4 \text{K}$, $\beta = -1.8$, $N_{\text{lim}} = 10^{11.3} \text{cm}^{-2}$ – yields $\Omega_{\text{Ly}\alpha} = 0.6\Omega_b$.

On empirical grounds alone, then, the current observations do not rule out a scenario where the photoionized Ly α forest contains most of the baryons not locked in denser phases, which we estimate at $\simeq 0.1\Omega_b$. This would require, however, a warmer IGM than predicted by numerical simulations and a $f(N_{\text{HI}}, X)$ function that remains steep to $N_{\text{HI}} \approx 10^{11} \text{cm}^{-2}$. The latter point may be tested with new observations of the IGM using the planned HST/COS instrument, especially if it achieves $\text{S/N} > 50$ per pixel. Given that the uncertainties must be pressed in concert to their limits for the budget to be complete, it is also reasonable to conclude that the IGM does not contain all of the missing baryons at $z \sim 0$. In the next section we will take up the question of what could fill this gap, assuming it exists.

6.6 The WHIM

In Figure 8, we present the $z \sim 0$ baryonic mass density estimates for the phases described in the previous sub-section. A simple summation of the central value estimate of each component⁵ yields a total $\Omega_{\text{stars}} + \Omega_{\text{H}_2} + \Omega_{\text{neut}} + \Omega_{\text{ICM}} + \Omega_{\text{Ly}\alpha} = 0.27\Omega_b$. Therefore, having followed the footsteps of FHP98, we reach a similar con-

⁵ Although there lies a gap in our knowledge of gas with $N_{\text{HI}} \approx 10^{17} \text{cm}^{-2}$, it is unlikely that this gas contributes significantly to Ω_b .

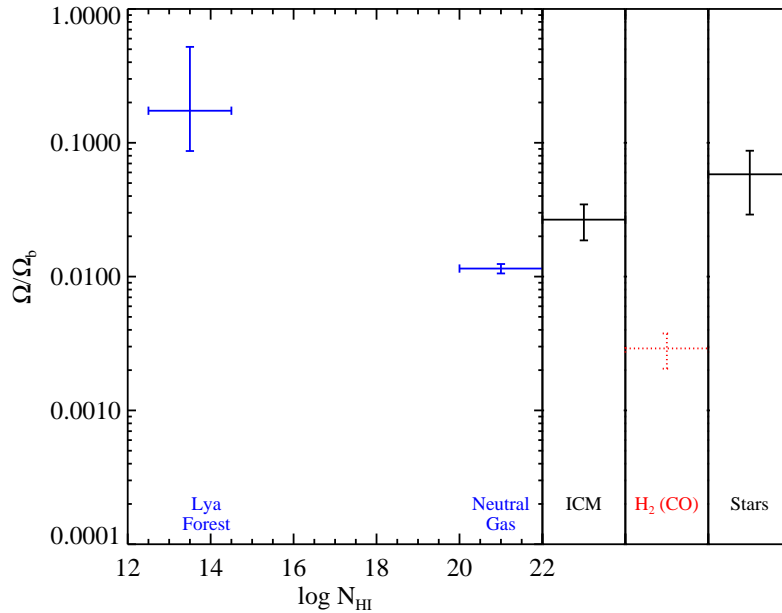


Fig. 8 Estimates of the baryonic mass density (relative to Ω_b) for various phases of baryons in the $z \sim 0$ universe. On the left side of the figure we show the mass densities estimated from the photoionized Ly α forest and the neutral gas in low z galaxies. One notes that the sum of the central values for the various components is significantly less than unity. This suggests that a significant mass component is missing from this census, e.g. the warm/hot intergalactic medium (WHIM). Even adopting the maximum values for each component, one may require an additional baryonic phase to contribute at $z = 0$.

clusion: current observations have not revealed roughly 70% of the baryons in the $z \sim 0$ universe. The observational techniques described in the previous section are sensitive to baryons in luminous matter, hot ($T > 10^7 \text{K}$) and diffuse gas, molecular and atomic neutral gas, and diffuse photoionized gas. From a practical standpoint, this leaves one obvious phase: warm/hot ($10^5 \text{K} < T < 10^7 \text{K}$), diffuse gas.

Indeed FHP98 identified this phase as the likely reservoir for the remainder of baryons and suggested it would be associated with galaxy groups and galactic halos (see also [85]). Cosmological simulations of the low redshift universe, meanwhile, argue that a warm/hot phase exists yet external to galaxies, i.e. within the intergalactic medium [18, 30]. This warm/hot intergalactic medium (WHIM), believed to be heated by shocks during large-scale gravitational collapse, is predicted by the simulations to comprise roughly 50% of baryons in the present universe. Bregman [13] has recently reviewed the observational and theoretical evidence for the WHIM at $z \sim 0$. We refer the reader to that manuscript for a broader discussion. We highlight here only a few points with emphasis on absorption-line observations.

The WHIM gas, as conceived in numerical simulations or as gas reservoirs of galaxy groups, has too low density and temperature to be detected in emission by

current X-ray instrumentation and even the next generation of X-ray facilities would be unlikely to detect the most diffuse gas. The neutral fraction, meanwhile, is far too low to permit detections via 21cm observations. For these reasons, searches for WHIM gas have essentially been limited to absorption-line techniques. The current approaches include (1) a search for the wisps of HI gas associated with the WHIM and (2) surveys for ions of O (and Ne) which trace warm/hot gas.

The first (and most popular) approach has been to survey intergalactic O^{+5} along quasar sightlines. This is primarily driven by observational efficiency; oxygen exhibits a strong OVI doublet at ultraviolet wavelengths (1031, 1037Å) that can be surveyed with high resolution, moderate signal-to-noise observations. To date, these have been acquired by spectrometers on the HST and FUSE satellites. In collisional ionization equilibrium (CIE; [50, 140]), the O^{+5} ion is abundant in gas with $T = 10^5$ to 10^6 K and therefore may trace the cooler WHIM. A hard radiation field, however, may also produce substantial O^{+5} ions in a diffuse gas. Therefore, the detection of OVI is not definitive proof of WHIM gas. Tripp and collaborators were the first to demonstrate that intergalactic OVI may be detected along quasar sightlines [146, 147]. Surveys along tens of sightlines have now been comprised with HST/STIS and FUSE observations [26, 27, 142, 148] which reveal a line density $\ell(z)$ of absorbers with equivalent width $W_{1031} \geq 50\text{mÅ}$ of $\ell(z) \approx 10$ absorbers per unit redshift path.

Intriguingly this incidence and the observed equivalent width distribution are in broad agreement with the predictions from $z \sim 0$ cosmological simulations [17]. At the least, this should be considered circumstantial evidence for WHIM gas. On the other hand, the majority of systems showing OVI absorption also exhibit coincident CIII absorption [28, 105]. The O^{+5} and C^{++} ions cannot coexist in CIE; their coincident detection either indicates a multi-phase medium or a photoionized gas. Tripp et al. [148] have also emphasized that $\approx 40\%$ of OVI absorbers show HI absorption with nearly identical line profile (Figure 9, see also [143]). In these cases, the observations suggest a gas temperature $T < 10^5$ K, i.e. photoionized material⁶. In other cases, the OVI absorption is offset in velocity from the strongest HI absorption and there is little diagnostic constraint on the gas temperature. In only a few cases (e.g. the $z = 0.1212$ absorber toward HS1821+643; [145]) does one detect broad $\text{Ly}\alpha$ absorption aligned with the OVI absorption that favors collisionally ionized gas with $T > 10^5$ K. It is our opinion, therefore, that the majority of OVI detections to date have not confirmed the presence of a major reservoir of $T > 10^5$ WHIM gas.

Furthermore, it is even premature to identify this gas with the intergalactic medium. Although the incidence of OVI absorbers is too high for all of them to be associated with the halos of $L \approx L^*$ galaxies, there are sufficient numbers of dwarf galaxies to locate the gas within their halos or “zones of metal enrichment” if these extend to ≈ 150 kpc [150]. Indeed, searches for galaxies linked with OVI absorbers have indicated a range of associations from individual galactic halos to galaxy groups to intergalactic gas [110, 138, 144, 152]. We await a larger statistical sample and detailed comparison to numerical simulations to resolve this issue [45].

⁶ Although one could invoke undetected, broad $\text{Ly}\alpha$ absorption in these cases, this would not predict the observed identical line-profiles for OVI and $\text{Ly}\alpha$ absorption.

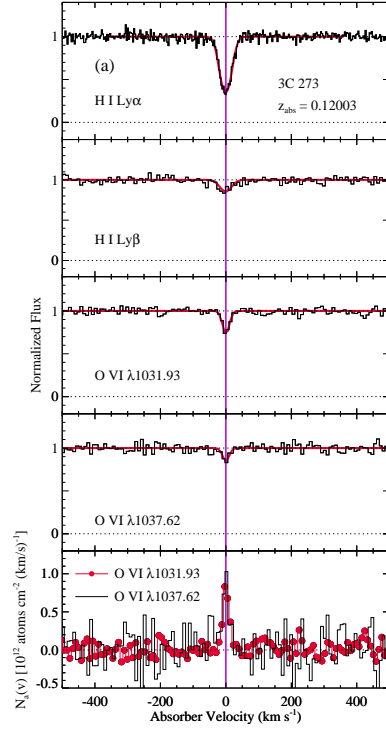


Fig. 9 Plot of the Ly α , Ly β , and OVI line-profiles for an OVI absorber at $z = 0.12$ toward 3C273 (taken from [148]). Note the high similarity between the OVI and HI profiles. This indicates the gas is not thermally broadened and requires a gas temperature $T < 10^5$ K. In turn, this implies the material is predominantly photoionized, not collisionally ionized and is therefore unlikely to correspond to warm/hot intergalactic gas. Roughly 40% of OVI absorbers share these properties. It remains an open question as to whether the majority of observed OVI gas corresponds to the WHIM.

Ignoring these concerns, one may speculate on the mass density of the OVI-bearing gas Ω_{OVI} using similar techniques as for the Ly α forest. Because OVI is simply a tracer of the material, one must assume both the metallicity and an ionization correction for the gas. Current estimations give $\Omega_{\text{OVI}} \approx 0.1\Omega_b$ [27]. Therefore, even in the case that the OVI-bearing gas traces only WHIM material, it is evident that it comprises a relatively small fraction of the baryon census.

Ideally, one would assess the mass density and spatial distribution of WHIM gas through observations of hydrogen which dominates the mass. This is, however, a difficult observational challenge. Assuming CIE, a WHIM ‘absorber’ with (an optimistic) total hydrogen column of $N_H = 10^{20} \text{ cm}^{-2}$ and $T = 10^6 \text{ K}$ will have an HI column density of $N_{\text{HI}} = 10^{13.5} \text{ cm}^{-2}$ and Doppler parameter $b_{\text{HI}} = 90 \text{ km s}^{-1} (T/10^6 \text{ K})^{1/2}$. This gives a peak optical depth $\tau_0 = 1.5 \times 10^{-2} (N\lambda_{\text{Ly}\alpha} f_{\text{Ly}\alpha}) / b_{\text{HI}} = 0.25$ and a total equivalent width $W_{\text{Ly}\alpha} = 150 \text{ m}\text{\AA}$. The detection of such a line-

profile requires at least moderate resolution UV spectra at relatively high S/N and also a precise knowledge of the intrinsic continuum of the background source.

Detections of line profiles consistent with broad Ly α absorption have now been reported in the few HST/STIS echelle spectra with high S/N [116]. Because these detections lie near the sensitivity limit of the spectra, it is not possible to exclude the possibility that these broad features arise from the blends of several weak, narrow absorbers. Furthermore, independent analysis of these same datasets have questioned at least several of the putative detections (Stoche, priv. comm.). These issues can only be resolved by higher S/N observations and, ideally, analysis of the corresponding Ly β profiles. We look forward to the installation of HST/COS which should enable such observations. Even if one can conclusively demonstrate the presence of warm/hot gas with broad Ly α absorbers, there are limitations to directly assessing the mass density of this gas from empirical observation. First, studies of numerical simulations reveal that broad Ly α lines arise from gas whose kinematics are a mixture of thermally and turbulently broadened motions making it difficult to derive the temperature and obtain an ionization correction [115]. Second, these same models predict that photoionization processes are significant for some gas with $T < 10^6$ K and this contribution to the ionization correction cannot be assessed from HI observations alone. Finally, the detection of broad Ly α features becomes prohibitive for gas with $T > 10^{6.5}$ K (i.e. $\tau_0 < 0.05$ for $N_H = 10^{20}$ cm $^{-2}$), which may account for the majority of WHIM material by mass (e.g. [30]). In short, one is driven to statistical comparisons between numerical simulations and observations of broad Ly α absorption and, ultimately, may be limited to a minor fraction of the WHIM.

At $T > 10^{6.3}$ K, the ion fraction of O $^{+5}$ is negligible and broad Ly α lines are generally too weak to detect with previous or planned UV spectrometers. To more efficiently trace this gas, we must turn to higher ionization states of oxygen and other elements. One option is the NeVIII doublet which probes gas to $T \approx 10^7$ K and is accessible with UV spectrometers for $z > 0.25$ [123]. The most sensitive tracers of $T > 10^6$ K gas, however, are resonance lines of OVII and OVIII. With current X-ray satellites, these observations are a demanding challenge; one is limited by both spectral resolution and instrument collecting area. Nicastro and collaborators have addressed the latter issue (in part) by monitoring X-ray variable sources that show occasional, bright flares. During a flare event, one obtains target-of-opportunity observations to yield a relatively high S/N dataset [39, 89, 162]. While this program has been successful observationally, the purported detections of intergalactic OVII and OVIII remain controversial [112]. While we are optimistic that these programs will reveal a few indisputable detections before the demise of the Chandra and XMM observatories, it is evident that a statistical survey for OVII and OVIII awaits future instrumentation (e.g. Con-X). Because OVI may indicate cooling gas within a hot medium (or hot-cold interfaces), the numerous detections of OVI can serve as signposts to the ‘true’ WHIM [130].

Ultimately, however, the challenge will remain to convert these tracers of hot gas into constraints on the mass density and spatial distribution of WHIM gas. At a

minimum, this requires assumptions about the metal-enrichment of the intergalactic medium.

In summary, we find the current empirical evidence for the WHIM to be intriguing but far from definitive. One must consider additional means for exploring the WHIM that would be enabled by new, proposed or planned instrumentation. One of these is to explore the line *emission* (e.g. $\text{Ly}\alpha$, OVI, OVII) from the denser WHIM gas [7, 17], which could be accomplished with UV and X-ray missions currently in design (e.g. *IGM, XENIA*). If combined with absorption-line studies, one may map out the mass density and spatial distribution of this gas at low z . Finally, it may be possible to cross-correlate the Sunyaev-Zeldovich (SZ) signal of the CMB with WHIM structures to infer the density and spatial distribution of this ionized gas [52]. This might be accomplished with currently planned SZ experiments.

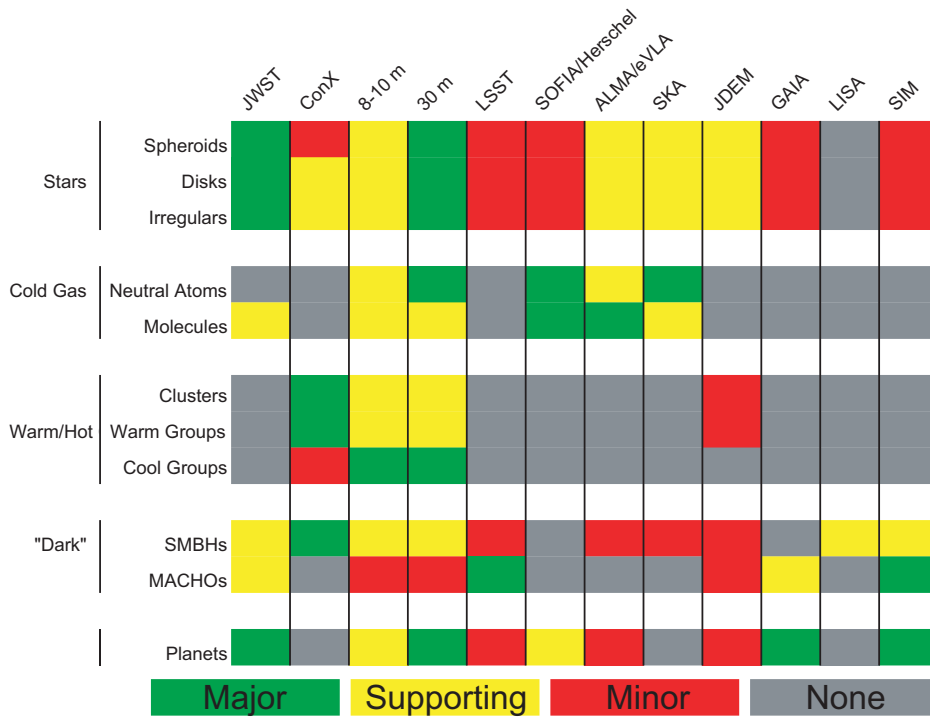


Fig. 10 For specific missions or categories of facility, the colors represent the role they are expected to play in measuring the budget of baryons in each phase discussed in the text.

7 Future Facilities and the Baryon Census

In the spirit of the meeting “Astrophysics in the Next Decade: JWST and Concurrent Facilities”, we consider how the baryon census will be advanced by the facilities in development now for operations in the next decade. To stimulate discussion at the conference, we composed a chart showing the applicability of each mission or facility to the important reservoirs of baryonic matter. The list of missions under consideration was obtained from the conference website. This chart appears in Figure 10, with the contributions of each mission color coded for major (green), supporting (yellow), minor (red), or no (grey) role. These assignments were made in the idiosyncratic judgment of one of us (J. T.) and should not be taken too literally. Each mission has its own, presumably compelling, scientific justification that in most cases does not explicitly include the baryon census (though JWST and Con-X are notable exceptions). The assignments were based primarily on wavelength coverage, spectral and spectroscopic resolution, field of view, and a review of the mission’s public science case where available.

The overlap between missions and baryonic components raise some interesting points. First, the future looks relatively bright for the baryon census as a whole. JWST, Con-X, and ALMA are the three most important missions for resolving uncertainties in the census of baryons in stars, hot gas, and cold gas respectively. These are the areas of greatest uncertainty today, so this is somewhat encouraging for the future. However, only two of these facilities are in development phases: Con-X is still under study and could not reasonably be expected to fly until late in the next decade or after 2020.

The “Assembly of Galaxies” is one of the four top-level science drivers of JWST, which will have the sensitivity and wavelength coverage to improve on stellar mass estimates at high redshift and the ability to measure IMFs by star counts over much larger local volumes than has been possible to date. As this is the most uncertain step in the derivation of the cosmic stellar mass budget, assessing the variation of the IMF from place to place and over time should be a primary goal of galaxy formation and evolution studies with JWST.

It looks as though the next decade will bring major advances in the study of the cold neutral and molecular phases of baryons over a wide redshift range, thanks to ALMA and eVLA. As mentioned above, the greatest need in this area is for a more thorough testing of the conversion factor from CO mass to H₂ mass in a broad range of astrophysical environments.

One pleasant surprise from this exercise is the notable versatility of large, ground-based optical telescopes (Keck and VLT today, and the 20 – 30 m ELTs in the future). Though they can lead the way for direct studies of stellar masses over a wide range of redshifts, they also support investigations whose primary use is in another wavelength range. Often this role requires them to obtain supporting data such as spectroscopic redshifts for high-*z* galaxies, optical counterparts for X-ray or radio sources, and the measurement of dynamical masses by high-resolution studies of linewidths in absorption or emission. It is likely that this versatility reflects the long history of optical astronomy, where the most mature technologies and techniques

are available, and their widespread availability compared with the scarce resource of space-based observing time.

This exercise also highlights a broad trend we may expect from astrophysics in the next decade. Since the baryon census encompasses many diverse astrophysical environments, from stars to the diffuse IGM, and requires a wide range of observational techniques, the capability of a facility to address the baryon census reflects its ability to address astrophysical problems in general. With this in mind, we note that many of the space missions in question are tailored to specific scientific questions rather than a broad, community-generated scientific program. While it is difficult to see how a mission like LISA could have collateral uses beyond the detection of gravity waves from a few astrophysical sources, even missions carrying more conventional instruments like JDEM, GAIA, and SIM are fine-tuned to specific scientific cases. This trend toward specialization, even among flagship-scale missions, will evidently be a hallmark of astrophysics in the next decade.

Finally, we note that perhaps the greatest need for new capabilities to address the “missing baryons” lies in the X-ray, and that there is no realistic chance for Con-X or something like it to launch before the very end of the next decade. Thus it is possible that astronomers will, by 2015, see the “first galaxies” (JWST), measure DE equation of state (LSST+JDEM), weigh molecules at $z \sim 6$ (ALMA), discover gravitational waves (LISA), find earthlike extrasolar planets (SIM+GAIA), and still not know where all the ordinary matter is or what phase it is in. This long interval would place the solution to the missing baryons problem at least 20 years away from when it was first recognized. This may be one of those cases where the urgency of performing an observation is tempered by the conventional wisdom that we already know the answer (the WHIM). But theory has been wrong before, and the only way to know is to do the experiment. If the last decade of astrophysics is a reliable guide, the next ten years will bring a few surprises. The what, when, and where of the baryons may well be among them.

Acknowledgements J. X. P. is partially supported by NASA/Swift grant NNX07AE94G and an NSF CAREER grant (AST-0548180). J. T. gratefully acknowledges the generous support of Gilbert and Jaylee Mead for their namesake fellowship in the Yale Center for Astronomy and Astrophysics.

References

- [1] Adelman-McCarthy, J. K., et al. 2007, *ApJS*, 172, 634
- [2] Aguirre, A., Hernquist, L., Schaye, J., Weinberg, D. H., Katz, N., & Gardner, J. 2001, *ApJ*, 560, 599
- [3] Allen, S. W., Rapetti, D. A., Schmidt, R. W., Ebeling, H., Morris, R. G., & Fabian, A. C. 2008, *MNRAS*, 383, 879
- [4] Becker, G. D., Rauch, M., & Sargent, W. L. W. 2007, *ApJ*, 662, 72
- [5] Bergeron, J., & Herbert-Fort, S. 2005, in *IAU Colloq. 199: Probing Galaxies through Quasar Absorption Lines*, ed. P. Williams, C.-G. Shu, & B. Menard,

265–280

- [6] Bernstein, R., Sheckman, S. A., Gunnels, S. M., Mochnacki, S., & Athey, A. E. 2003, in *Instrument Design and Performance for Optical/Infrared Ground-based Telescopes*. Edited by Iye, Masanori; Moorwood, Alan F. M. *Proceedings of the SPIE*, Volume 4841, pp. 1694-1704 (2003), 1694–1704
- [7] Bertone, S., Schaye, J., & Dolag, K. 2008, *Space Science Reviews*, 134, 295
- [8] Blanton, M. R., et al. 2003, *ApJ*, 592, 819
- [9] Boesgaard, A. M., Stephens, A., & Deliyannis, C. P. 2005, *ApJ*, 633, 398
- [10] Bolton, J. S., Haehnelt, M. G., Viel, M., & Springel, V. 2005, *MNRAS*, 357, 1178
- [11] Bouché, N., Gardner, J. P., Katz, N., Weinberg, D. H., Davé, R., & Lowenthal, J. D. 2005, *ApJ*, 628, 89
- [12] Bouché, N., Lehnert, M. D., & Péroux, C. 2006, *MNRAS*, 367, L16
- [13] Bregman, J. N. 2007, *ARAA*, 45, 221
- [14] Briggs, F. H., & Wolfe, A. M. 1983, *ApJ*, 268, 76
- [15] Bryan, G. L., Machacek, M., Anninos, P., & Norman, M. L. 1999, *ApJ*, 517, 13
- [16] Burles, S., & Tytler, D. 1998, *ApJ*, 507, 732
- [17] Cen, R., & Fang, T. 2006, *ApJ*, 650, 573
- [18] Cen, R., & Ostriker, J. P. 1999, *ApJ*, 514, 1
- [19] Chapman, S. C., Blain, A. W., Smail, I., & Ivison, R. J. 2005, *ApJ*, 622, 772
- [20] Chelouche, D., Ménard, B., Bowen, D. V., & Gnat, O. 2007, *ArXiv e-prints*, 706
- [21] Chen, H.-W., Prochaska, J. X., Bloom, J. S., & Thompson, I. B. 2005, *ApJL*, 634, L25
- [22] Chen, H.-W., Prochaska, J. X., & Gnedin, N. Y. 2007, *ApJL*, 667, L125
- [23] Cole, S., et al. 2001, *MNRAS*, 326, 255
- [24] Cooke, J., Wolfe, A. M., Gawiser, E., & Prochaska, J. X. 2006, *ApJL*, 636, L9
- [25] Cui, J., Bechtold, J., Ge, J., & Meyer, D. M. 2005, *ApJ*, 633, 649
- [26] Danforth, C. W., & Shull, J. M. 2005, *ApJ*, 624, 555
- [27] —. 2007, *ArXiv e-prints*, 709
- [28] Danforth, C. W., Shull, J. M., Rosenberg, J. L., & Stocke, J. T. 2006, *ApJ*, 640, 716
- [29] Davé, R. 2008, *MNRAS*, 385, 147
- [30] Davé, R., Cen, R., Ostriker, J. P., Bryan, G. L., Hernquist, L., Katz, N., Weinberg, D. H., Norman, M. L., & O’Shea, B. 2001, *ApJ*, 552, 473
- [31] Davé, R., Hernquist, L., Katz, N., & Weinberg, D. H. 1999, *ApJ*, 511, 521
- [32] Davé, R., & Tripp, T. M. 2001, *ApJ*, 553, 528
- [33] Dekel, A., & Birnboim, Y. 2006, *MNRAS*, 368, 2
- [34] Devereux, N. A., & Young, J. S. 1990, *ApJ*, 359, 42
- [35] Draine, B. T. 2006, in *Astronomical Society of the Pacific Conference Series*, Vol. 348, *Astrophysics in the Far Ultraviolet: Five Years of Discovery with FUSE*, ed. G. Sonneborn, H. W. Moos, & B.-G. Andersson, 58–+
- [36] Dunkley, J., et al. 2008, *ArXiv e-prints*, 803

- [37] Ellison, S. L., Yan, L., Hook, I. M., Pettini, M., Wall, J. V., & Shaver, P. 2001, *A & A*, 379, 393
- [38] Fall, S. M., & Pei, Y. C. 1993, *ApJ*, 402, 479
- [39] Fang, T., Marshall, H. L., Lee, J. C., Davis, D. S., & Canizares, C. R. 2002, *ApJL*, 572, L127
- [40] Faucher-Giguere, C. ., Prochaska, J. X., Lidz, A., Hernquist, L., & Zaldarriaga, M. 2007, *ArXiv e-prints*, 709
- [41] Fontana, A., et al. 2006, *A & A*, 459, 745
- [42] Fox, A. J., Petitjean, P., Ledoux, C., & Srianand, R. 2007, *A & A*, 465, 171
- [43] Fukugita, M. 2004, in *IAU Symposium*, Vol. 220, *Dark Matter in Galaxies*, ed. S. Ryder, D. Pisano, M. Walker, & K. Freeman, 227–+
- [44] Fukugita, M., Hogan, C. J., & Peebles, P. J. E. 1998, *ApJ*, 503, 518
- [45] Ganguly, R., Cen, R., Fang, T., & Sembach, K. 2008, *ArXiv e-prints*, 803
- [46] Gardner, J. P., Katz, N., Hernquist, L., & Weinberg, D. H. 2001, *ApJ*, 559, 131
- [47] Gawiser, E., et al. 2007, *ApJ*, 671, 278
- [48] Ge, J., & Bechtold, J. 1997, *ApJL*, 477, L73+
- [49] Giovanelli, R., et al. 2005, *AJ*, 130, 2598
- [50] Gnat, O., & Sternberg, A. 2007, *ApJS*, 168, 213
- [51] Haardt, F., & Madau, P. 1996, *ApJ*, 461, 20
- [52] Ho, S., Hirata, C. M., Padmanabhan, N., Seljak, U., & Bahcall, N. 2008, *ArXiv e-prints*, 801
- [53] Hoopes, C. G., Sembach, K. R., Heckman, T. M., Meurer, G. R., Aloisi, A., Calzetti, D., Leitherer, C., & Martin, C. L. 2004, *ApJ*, 612, 825
- [54] Hopkins, A. M., Rao, S. M., & Turnshek, D. A. 2005, *ApJ*, 630, 108
- [55] Hopkins, P. F., Richards, G. T., & Hernquist, L. 2007, *ApJ*, 654, 731
- [56] Hu, E. M., Kim, T.-S., Cowie, L. L., Songaila, A., & Rauch, M. 1995, *AJ*, 110, 1526
- [57] Jedamzik, K. 2004, *PhRD*, 70, 083510
- [58] Jena, T., Norman, M. L., Tytler, D., Kirkman, D., Suzuki, N., Chapman, A., Melis, C., Paschos, P., O’Shea, B., So, G., Lubin, D., Lin, W.-C., Reimers, D., Janknecht, E., & Fechner, C. 2005, *MNRAS*, 361, 70
- [59] Jenkins, A., Frenk, C. S., White, S. D. M., Colberg, J. M., Cole, S., Evrard, A. E., Couchman, H. M. P., & Yoshida, N. 2001, *MNRAS*, 321, 372
- [60] Jenkins, E. B., Tripp, T. M., Woźniak, P. R., Sofia, U. J., & Sonneborn, G. 1999, *ApJ*, 520, 182
- [61] Jorgenson, R. A., Wolfe, A. M., Prochaska, J. X., Lu, L., Howk, J. C., Cooke, J., Gawiser, E., & Gelino, D. M. 2006, *ApJ*, 646, 730
- [62] Kanekar, N., & Chengalur, J. N. 2003, *A & A*, 399, 857
- [63] Kauffmann, G., et al. 2003, *MNRAS*, 341, 33
- [64] Kawata, D., & Rauch, M. 2007, *ApJ*, 663, 38
- [65] Keres, D., Yun, M. S., & Young, J. S. 2003, *ApJ*, 582, 659
- [66] Kereš, D., Katz, N., Weinberg, D. H., & Davé, R. 2005, *MNRAS*, 363, 2
- [67] Kim, T.-S., Bolton, J. S., Viel, M., Haehnelt, M. G., & Carswell, R. F. 2007, *MNRAS*, 382, 1657

- [68] Kim, T.-S., Carswell, R. F., Cristiani, S., D'Odorico, S., & Giallongo, E. 2002, *MNRAS*, 335, 555
- [69] Kirkman, D., & Tytler, D. 1997, *ApJ*, 484, 672
- [70] Kirkman, D., Tytler, D., Suzuki, N., O'Meara, J. M., & Lubin, D. 2003, *ApJS*, 149, 1
- [71] Kohler, K., & Gnedin, N. Y. 2007, *ApJ*, 655, 685
- [72] Korn, A. J., Grundahl, F., Richard, O., Barklem, P. S., Mashonkina, L., Collet, R., Piskunov, N., & Gustafsson, B. 2006, *Nature*, 442, 657
- [73] Kriek, M., et al. 2006, *ApJL*, 649, L71
- [74] Kriss, G. A., et al. 2001, *Science*, 293, 1112
- [75] Lah, P., et al. 2007, *MNRAS*, 376, 1357
- [76] Le Floch, E., et al. 2003, *A & A*, 400, 499
- [77] Ledoux, C., Petitjean, P., & Srianand, R. 2003, *MNRAS*, 346, 209
- [78] Linsky, J. L., et al. 2006, *ApJ*, 647, 1106
- [79] McDonald, P., et al. 2006, *ApJS*, 163, 80
- [80] Meiksin, A., & White, M. 2003, *MNRAS*, 342, 1205
- [81] Meiksin, A. A. 2007, *ArXiv e-prints*, 711
- [82] Meyer, M. J., et al. 2004, *MNRAS*, 350, 1195
- [83] Miralda-Escudé, J., Cen, R., Ostriker, J. P., & Rauch, M. 1996, *ApJ*, 471, 582
- [84] Moos, H. W., et al. 2002, *ApJS*, 140, 3
- [85] Mulchaey, J. S., Davis, D. S., Mushotzky, R. F., & Burstein, D. 1996, *ApJ*, 456, 80
- [86] Murphy, M. T., & Liske, J. 2004, *MNRAS*, 354, L31
- [87] Nagamine, K., Wolfe, A. M., Hernquist, L., & Springel, V. 2007, *ApJ*, 660, 945
- [88] Netterfield, C. B., et al. 2002, *ApJ*, 571, 604
- [89] Nicastro, F., Mathur, S., Elvis, M., Drake, J., Fang, T., Fruscione, A., Krongold, Y., Marshall, H., Williams, R., & Zezas, A. 2005, *Nature*, 433, 495
- [90] Noterdaeme, P., Ledoux, C., Petitjean, P., & Srianand, R. 2008, *ArXiv e-prints*, 801
- [91] O'Meara, J. M., Prochaska, J. X., Burles, S., Prochter, G., Bernstein, R. A., & Burgess, K. M. 2007, *ApJ*, 656, 666
- [92] Ostriker, J. P., & Heisler, J. 1984, *ApJ*, 278, 1
- [93] Paschos, P., Jena, T., Tytler, D., Kirkman, D., & Norman, M. L. 2008, *ArXiv e-prints*, 802
- [94] Peimbert, M., Luridiana, V., & Peimbert, A. 2007, *ApJ*, 666, 636
- [95] Penton, S. V., Stocke, J. T., & Shull, J. M. 2002, *ApJ*, 565, 720
- [96] —. 2004, *ApJS*, 152, 29
- [97] Péroux, C., Dessauges-Zavadsky, M., D'Odorico, S., Kim, T.-S., & McMahon, R. G. 2003, *MNRAS*, 345, 480
- [98] —. 2007, *MNRAS*, 382, 177
- [99] Péroux, C., McMahon, R. G., Storrie-Lombardi, L. J., & Irwin, M. J. 2003, *MNRAS*, 346, 1103
- [100] Petitjean, P., Srianand, R., & Ledoux, C. 2000, *A & A*, 364, L26

- [101] Petitjean, P., Webb, J. K., Rauch, M., Carswell, R. F., & Lanzetta, K. 1993, *MNRAS*, 262, 499
- [102] Pettini, M., Smith, L. J., Hunstead, R. W., & King, D. L. 1994, *ApJ*, 426, 79
- [103] Prochaska, J. X. 1999, *ApJL*, 511, L71
- [104] Prochaska, J. X., & Burles, S. M. 1999, *AJ*, 117, 1957
- [105] Prochaska, J. X., Chen, H.-W., Howk, J. C., Weiner, B. J., & Mulchaey, J. 2004, *ApJ*, 617, 718
- [106] Prochaska, J. X., Gawiser, E., Wolfe, A. M., Castro, S., & Djorgovski, S. G. 2003, *ApJL*, 595, L9
- [107] Prochaska, J. X., Herbert-Fort, S., & Wolfe, A. M. 2005, *ApJ*, 635, 123
- [108] Prochaska, J. X., O'Meara, J. M., Herbert-Fort, S., Burles, S., Prochter, G. E., & Bernstein, R. A. 2006, *ApJL*, 648, L97
- [109] Prochaska, J. X., Tripp, T. M., & Howk, J. C. 2005, *ApJL*, 620, L39
- [110] Prochaska, J. X., Weiner, B. J., Chen, H.-W., & Mulchaey, J. S. 2006, *ApJ*, 643, 680
- [111] Rao, S. M., Turnshek, D. A., & Nestor, D. B. 2006, *ApJ*, 636, 610
- [112] Rasmussen, A. P., Kahn, S. M., Paerels, F., Herder, J. W. d., Kaastra, J., & de Vries, C. 2007, *ApJ*, 656, 129
- [113] Reddy, N. A., Steidel, C. C., Pettini, M., Adelberger, K. L., Shapley, A. E., Erb, D. K., & Dickinson, M. 2007, *ArXiv e-prints*, 706
- [114] Reiprich, T. H., & Böhringer, H. 2002, *ApJ*, 567, 716
- [115] Richter, P., Fang, T., & Bryan, G. L. 2006, *A & A*, 451, 767
- [116] Richter, P., Savage, B. D., Sembach, K. R., & Tripp, T. M. 2006, *A & A*, 445, 827
- [117] Rines, K., Diaferio, A., & Natarajan, P. 2008, *ArXiv e-prints*, 803
- [118] Rogerson, J. B., & York, D. G. 1973, *ApJL*, 186, L95+
- [119] Rosenberg, J. L., & Schneider, S. E. 2002, *ApJ*, 567, 247
- [120] Rudnick, G., Labbé, I., Förster Schreiber, N. M., Wuyts, S., Franx, M., Finlator, K., Kriek, M., Moorwood, A., Rix, H.-W., Röttgering, H., Trujillo, I., van der Wel, A., van der Werf, P., & van Dokkum, P. G. 2006, *ApJ*, 650, 624
- [121] Ryan-Weber, E. V., Webster, R. L., & Staveley-Smith, L. 2003, *MNRAS*, 343, 1195
- [122] Savage, B. D., Bohlin, R. C., Drake, J. F., & Budich, W. 1977, *ApJ*, 216, 291
- [123] Savage, B. D., Lehner, N., Wakker, B. P., Sembach, K. R., & Tripp, T. M. 2005, *ApJ*, 626, 776
- [124] Schaye, J. 2001, *ApJ*, 559, 507
- [125] —. 2001, *ApJL*, 559, L1
- [126] Schaye, J., Aguirre, A., Kim, T.-S., Theuns, T., Rauch, M., & Sargent, W. L. W. 2003, *ApJ*, 596, 768
- [127] Scott, J., Bechtold, J., Dobrzycki, A., & Kulkarni, V. P. 2000, *ApJS*, 130, 67
- [128] Sembach, K. R., et al. 2005, in *Bulletin of the American Astronomical Society*, Vol. 37, *Bulletin of the American Astronomical Society*, 1197–+
- [129] Shapley, A. E., Steidel, C. C., Pettini, M., Adelberger, K. L., & Erb, D. K. 2006, *ApJ*, 651, 688
- [130] Shull, J. M., Tumlinson, J., & Giroux, M. L. 2003, *ApJL*, 594, L107

- [131] Shull, J. M., Tumlinson, J., Giroux, M. L., Kriss, G. A., & Reimers, D. 2004, *ApJ*, 600, 570
- [132] Siana, B., Teplitz, H. I., Colbert, J., Ferguson, H. C., Dickinson, M., Brown, T. M., Conselice, C. J., de Mello, D. F., Gardner, J. P., Giavalisco, M., & Menanteau, F. 2007, *ApJ*, 668, 62
- [133] Simcoe, R. A., Sargent, W. L. W., & Rauch, M. 2002, *ApJ*, 578, 737
- [134] Simcoe, R. A., Sargent, W. L. W., Rauch, M., & Becker, G. 2006, *ApJ*, 637, 648
- [135] Spergel, D. N., et al. 2007, *ApJS*, 170, 377
- [136] Spite, M., Spite, F., & Maillard, J. P. 1984, *A & A*, 141, 56
- [137] Spitzer, L. 1978, *Physical processes in the interstellar medium* (New York Wiley-Interscience, 1978. 333 p.)
- [138] Stocke, J. T., Penton, S. V., Danforth, C. W., Shull, J. M., Tumlinson, J., & McLin, K. M. 2006, *ApJ*, 641, 217
- [139] Storrie-Lombardi, L. J., McMahon, R. G., Irwin, M. J., & Hazard, C. 1994, *ApJL*, 427, L13
- [140] Sutherland, R. S., & Dopita, M. A. 1993, *ApJS*, 88, 253
- [141] Tacconi, L. J., et al. 2006, *ApJ*, 640, 228
- [142] Thom, C., & Chen, H.-W. 2008, *ArXiv e-prints*, 801
- [143] —. 2008, *ArXiv e-prints*, 801
- [144] Tripp, T. M., Aracil, B., Bowen, D. V., & Jenkins, E. B. 2006, *ApJL*, 643, L77
- [145] Tripp, T. M., Giroux, M. L., Stocke, J. T., Tumlinson, J., & Oegerle, W. R. 2001, *ApJ*, 563, 724
- [146] Tripp, T. M., & Savage, B. D. 2000, *ApJ*, 542, 42
- [147] Tripp, T. M., Savage, B. D., & Jenkins, E. B. 2000, *ApJL*, 534, L1
- [148] Tripp, T. M., Sembach, K. R., Bowen, D. V., Savage, B. D., Jenkins, E. B., Lehner, N., & Richter, P. 2007, *ArXiv e-prints*, 706
- [149] Tumlinson, J. 2007, *ApJL*, 664, L63
- [150] Tumlinson, J., & Fang, T. 2005, *ApJL*, 623, L97
- [151] Tumlinson, J., Prochaska, J. X., Chen, H.-W., Dessauges-Zavadsky, M., & Bloom, J. S. 2007, *ApJ*, 668, 667
- [152] Tumlinson, J., Shull, J. M., Giroux, M. L., & Stocke, J. T. 2005, *ApJ*, 620, 95
- [153] Tumlinson, J., Shull, J. M., Rachford, B. L., Browning, M. K., Snow, T. P., Fullerton, A. W., Jenkins, E. B., Savage, B. D., Crowther, P. A., Moos, H. W., Sembach, K. R., Sonneborn, G., & York, D. G. 2002, *ApJ*, 566, 857
- [154] van Dokkum, P. G. 2008, *ApJ*, 674, 29
- [155] Viegas, S. M. 1995, *MNRAS*, 276, 268
- [156] Vladilo, G., Prochaska, J. X., & Wolfe, A. M. 2008, *A & A*, 478, 701
- [157] Vreeswijk, P. M., et al. 2004, *A & A*, 419, 927
- [158] Walter, F., Bertoldi, F., Carilli, C., Cox, P., Lo, K. Y., Neri, R., Fan, X., Omont, A., Strauss, M. A., & Menten, K. M. 2003, *Nature*, 424, 406
- [159] Weymann, R. J., et al. 1998, *ApJ*, 506, 1
- [160] Weymann, R. J., Vogel, S. N., Veilleux, S., & Epps, H. W. 2001, *ApJ*, 561, 559

- [161] White, R. L., Becker, R. H., Fan, X., & Strauss, M. A. 2003, *AJ*, 126, 1
- [162] Williams, R. J., Mathur, S., & Nicastro, F. 2006, *ApJ*, 645, 179
- [163] Wolfe, A. M., Gawiser, E., & Prochaska, J. X. 2005, *ARAA*, 43, 861
- [164] Wolfe, A. M., Turnshek, D. A., Smith, H. E., & Cohen, R. D. 1986, *ApJS*, 61, 249
- [165] Young, J. S., & Scoville, N. Z. 1991, *ARAA*, 29, 581
- [166] Zwaan, M. A., Briggs, F. H., Sprayberry, D., & Sorar, E. 1997, *ApJ*, 490, 173
- [167] Zwaan, M. A., Meyer, M. J., Staveley-Smith, L., & Webster, R. L. 2005, *MNRAS*, 359, L30
- [168] Zwaan, M. A., & Prochaska, J. X. 2006, *ApJ*, 643, 675
- [169] Zwaan, M. A., van der Hulst, J. M., Briggs, F. H., Verheijen, M. A. W., & Ryan-Weber, E. V. 2005, *MNRAS*, 364, 1467